Subgrid-scale modelling for large-eddy simulation including scalar mixing in rotating turbulent shear flows

by

Linus Marstorp

April 2006
Technical Reports from
Royal Institute of Technology
KTH Mechanics
SE-100 44 Stockholm, Sweden

Akademisk avhandling som med tillstånd av Kungliga Tekniska Högskolan i Stockholm framlägges till offentlig granskning för avläggande av teknologie licentiatexamen fredagen den 28 april 2006 kl 13.30 i sal D3, Kungliga Tekniska Högskolan, Vallhallavägen 79, Stockholm.

Universitetsservice US–AB, Stockholm 2006

Subgrid-scale modelling for large-eddy simulation including scalar mixing in rotating turbulent shear flows

Linus Marstorp
KTH Mechanics, SE-100 44 Stockholm, Sweden

Abstract

The aim of the present study is to develop subgrid-scale models that are relevant for complex flows and combustion. A stochastic model based on a stochastic Smagorinsky constant with adjustable variance and time scale is proposed. The stochastic model is shown to provide for backscatter of both kinetic energy and scalar variance without causing numerical instabilities. A new subgrid-scale scalar flux model is developed using the same kind of methodology that leads to the explicit algebraic scalar flux model, EASFM, for RANS. The new model predicts the anisotropy of the subgrid-scales in a more realistic way than the eddy diffusion model. Both new models were tested in rotating homogeneous shear flow with a passive scalar. Rogallo's method of moving the frame with the mean flow to enable periodic boundary conditions was used to simulate homogeneous shear flow.

Descriptors: Turbulence, large-eddy simulation, subgrid-scale model.

Preface

The thesis contains the following papers:

Paper 1. Linus Marstorp, Geert Brethouwer & Arne V. Johansson. *Stochastic SGS modelling in rotating homogeneous shear flow with a passive scalar.* To be submitted

Paper 2. Linus Marstorp, Geert Brethouwer & Arne V. Johansson. *A new model for the subgrid passive scalar flux.* To be submitted

Paper 3. Linus Marstorp, Geert Brethouwer & Arne V. Johansson. *A code for large eddy simulation of rotating homogeneous shear flow with passive scalars.* Technical report

Division of work between authors

The project was initiated and defined by Arne Johansson and Geert Brethouwer. The work was performed by Linus Marstorp under the supervision of Arne Johansson and Geert Brethouwer. The large eddy simulations were performed by Marstorp. The papers were written by Linus Marstorp and reviewed by Arne Johansson and Geert Brethouwer.

Contents

CHAPTER 1

Introduction

The nature of turbulent flows is chaotic and three-dimensional with a wide range of the scales of motion. Predictions of (Newtonian) turbulent flows require numerical solution of the Navier-Stokes equation. Unfortunately, direct numerical simulations of the Navier-Stokes equations demand very high resolution. All scales, even the smallest scales of motion, have to be resolved in order to capture the correct physics of the flow. A less computationally expensive approach is to solve the Navier-Stokes equations in the mean sense. This is usually referred to as a Reynolds averaged Navier-Stokes, RANS, approach. The RANS approach provides for mean statistics, such as the mean velocity profile and the mean turbulence kinetic energy, but all turbulent fluctuations have to be modelled. The subject for this study is a third approach; Large Eddy Simulation, LES, which captures the dynamics of the largest turbulence length scales and only requires modelling of the smallest scales of motion.

The aim of the present study is develop models for LES with passive scalars. A passive scalar is mixed by the flow, but it has no effect on the flow. It can represent, for example, small temperature fluctuations or a pollutant carried by the flow. Knowledge of passive scalar mixing is also a first step towards the understanding of reactive flows, where the mixing of species plays an important role. At a later stage, the LES models will be implemented in codes for numerical simulations of turbulent flows in complex geometries, such as the wall-jet code developed by Ahlman et al. (2006)

CHAPTER 2

Filtered equations

A Large Eddy Simulation is an under-resolved numerical simulation of the Navier-Stokes equations in which only the large length and time scales are resolved, and in which the influence of the non-resolved scales has to be modelled. To remove the scales smaller than a prescribed filter scale Δ, a filtering operation is applied to the Navier-Stokes equation. The filter can be represented by a convolution

$$\tilde{u}(\mathbf{x},t) = \int_{\mathbb{R}^3} G(\mathbf{x}-\mathbf{y})u(\mathbf{y},t)d\mathbf{y} \tag{2.1}$$

which commutes with the differential operator. The filtered Navier-Stokes equations are

$$\begin{aligned}
&\frac{\partial \tilde{u}_i}{\partial t} + \tilde{u}_j\frac{\partial \tilde{u}_i}{\partial x_j} = -\frac{1}{\rho}\frac{\partial \tilde{p}}{\partial x_i} + \nu\nabla^2\tilde{u}_i - \frac{\partial \tau_{ij}}{\partial x_j} \\
&\frac{\partial \tilde{u}_i}{\partial x_i} = 0 \\
&\frac{\partial \tilde{\theta}}{\partial t} + \tilde{u}_j\frac{\partial \tilde{\theta}}{\partial x_j} = \frac{\nu}{Pr}\nabla^2\tilde{\theta} - \frac{\partial q_j}{\partial x_j}
\end{aligned} \tag{2.2}$$

where $\tilde{u}_i$ and $\tilde{\theta}$ denote the filtered velocity and passive scalar respectively, and $\tilde{p}$ is the pressure. Ω_i is the system rotation vector, ν is the viscosity, and Pr is the Prandtl number. The sub-grid scale, SGS, stress, $\tau_{ij} = \widetilde{u_iu_j} - \tilde{u}_i\tilde{u}_j$, and the SGS scalar flux, $q_i = \widetilde{u_i\theta} - \tilde{u}_i\tilde{\theta}$, have to be modelled in order to close the system of equations.

CHAPTER 3

Important features of τ_{ij} and q_j

In incompressible turbulent flows kinetic energy is produced by the mean velocity gradients (shear). The kinetic energy is then transferred from large energetic eddies to smaller eddies through an energy cascade governed by nonlinear interactions. The viscous forces become important at the smallest scales of motion. They dampen the turbulent fluctuations and kinetic energy is dissipated. In LES, the dissipative scales are not resolved and modelling is needed in order to produce an energy cascade. One of the basic demands on an SGS model is that it produces the correct amount of mean energy and scalar variance dissipation. Thereby the mean turbulence kinetic energy and the scalar variance develop in a proper manner. The energy cascade in LES is sketched in figure 3.1.

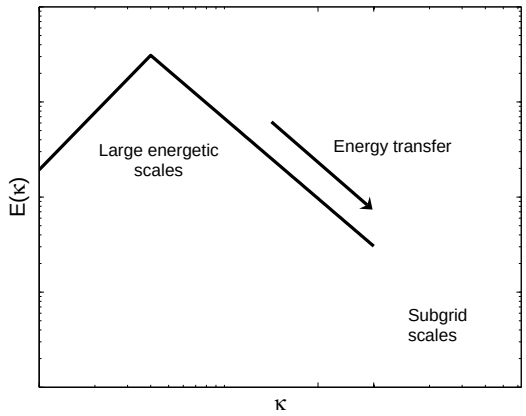

FIGURE 3.1. *Sketch of the kinetic energy spectrum $E(\kappa)$ in LES.*

Although the energy transfer, or SGS dissipation, is positive on average, it varies spatially and temporary with intermittently negative values. Negative SGS dissipation is referred to as backscatter, and it is significant in turbulent flows, see Piomelii et al. (1991) or Cerutti and Meneveau (1998). Piomelli et al. found the probability of backscatter to be approximately 50% in turbulent channel flow.

A realistic description of the energy transfer between the resolved and SGS also involves a proper description of the anisotropy of the mean energy transfer. Experiments by Kang and Meneveau (2001) have shown that the mean kinetic energy transfer becomes isotropic, i.e. equal in all directions, whereas the mean scalar 'energy' transfer stays anisotropic when the filter scale is decreased. A correct description of the anisotropy of the energy transfer requires advanced SGS modelling.

CHAPTER 4

Subgrid scale models

SGS models for LES are in general simpler than Reynolds stress models for RANS with reference to the number of transport equations involved. Most SGS models belong to the class of zero-equation models. However, the resolved velocity and scalar fields in LES provide valuable information that can be used to improve the model predictions.

4.1. The Smagorinsky model

The widely known Smagorinsky (1962) model is an eddy viscosity model which reads

$$\tau_{ij} = -2\nu_T S_{ij} \tag{4.3}$$

where S_{ij} is the resolved rate of strain and where the eddy viscosity, ν_T, is constructed from the filter length scale Δ and a velocity scale $\Delta|S_{ij}|$, such that

$$\nu_T = (C_s\Delta)^2|S_{ij}| \tag{4.4}$$

where $|S_{ij}| = (2S_{ij}S_{ij})^{1/2}$ and $C_s > 0$ is a model constant. The model is stable and computationally inexpensive. Moreover, a constant Smagorinsky constant, C_s, is consistent with the Kolmogorov theory for the energy cascade in isotropic turbulent flows Pope (2000). However, the Smagorinsky model has several known deficiencies. One example is that with $C_s > 0$ the SGS-dissipation is strictly positive, i.e. there is no backscatter. Another example is that the model constant has to be damped in near wall regions. The latter problem is also associated with eddy viscosity models for RANS.

The corresponding SGS model for the passive scalar is the eddy diffusion model

$$q_i = -\frac{\nu_T}{Pr_T}\frac{\partial\tilde{\theta}}{\partial x_i} \tag{4.5}$$

Like the Smagorinsky model, the eddy diffusion model does not provide for backscatter. Another deficiency is its inability to predict the anisotropy of the scalar variance SGS dissipation, as pointed out by Kang and Meneveau (2001).

4.2. Dynamic Smagorinsky model

In the dynamic Smagorinsky model developed by Germano et al. (1991), information about the resolved scales is used to estimate the Smagorinsky constant.

According to the Germano identity the difference between the SGS stress evaluated at two different filter scales is

$$\tau_{ij}^{\hat{\Delta}} - \widehat{\tau_{ij}^{\Delta}} = \widehat{\tilde{u}_i \tilde{u}_j} - \hat{\tilde{u}}_i \hat{\tilde{u}}_j \tag{4.6}$$

where the hat operator denotes an explicit test filter at larger filter width, $\hat{\Delta} > \Delta$. By replacing the real SGS stress by the modelled stress and by assuming scale invariance of the Smagorinsky constant the following relation is obtained

$$-2C_s^2 \left(\hat{\Delta}^2 |\hat{\tilde{S}}| \hat{\tilde{S}}_{ij} - \Delta^2 \widehat{|\tilde{S}| \tilde{S}_{ij}} \right) = \widehat{\tilde{u}_i \tilde{u}_j} - \hat{\tilde{u}}_i \hat{\tilde{u}}_j \tag{4.7}$$

Germano originally proposed to compute the model constant as

$$\begin{aligned} C_s^2 &= \frac{\langle L_{ij} \tilde{S}_{ij} \rangle}{\langle M_{ij} \tilde{S}_{ij} \rangle} \\ L_{ij} &= \widehat{\tilde{u}_i \tilde{u}_j} - \hat{\tilde{u}}_i \hat{\tilde{u}}_j \\ M_{ij} &= -2(\hat{\Delta}^2 |\hat{\tilde{S}}| \hat{\tilde{S}}_{ij} - \Delta^2 \widehat{|\tilde{S}| \tilde{S}_{ij}}) \end{aligned} \tag{4.8}$$

where the brackets $\langle\rangle$ denote averaging in homogeneous directions. Lilly (1992) proposed the more widely used procedure, $C_s^2 = \langle L_{ij} M_{ij} \rangle / \langle M_{ij} M_{ij} \rangle$, which is a least-square solution to (4.7) minimising the error $\langle L_{ij} - C_s^2 M_{ij} \rangle$.

Averaging in homogeneous directions according to (4.7) is not possible in complex geometries that lack such directions. In that case, time averaging is an option, but it is not consistent with Galilean invariance unless it is implemented in a Lagrangian frame of reference. Meneveau et al. (1996) developed such a Lagrangian dynamic model with averaging along path lines. Without the averaging the dynamic model provides for backscatter but the model constant yields excessively large fluctuations and it can easily become unstable.

With the dynamic approach, the Smagorinsky constant is adjusted to the local flow conditions. The model provides for a correct near wall scaling, and it can be applied to flows containing both laminar and turbulent regions. Variations of the dynamic approach have been applied to a wide range of SGS models. A recent example is the three coefficient nonlinear dynamic model developed by Wang and Bergstrom (2005).

4.3. Scale similarity model

In the scale similarity model developed by Bardina et al. (1983), the SGS stress is assumed to be similar to the one constructed by the resolved velocity field and an explicit test filter with equal or larger filter scale

$$\tau_{ij} = \widehat{\tilde{u}_i \tilde{u}_j} - \hat{\tilde{u}}_i \hat{\tilde{u}}_j \tag{4.9}$$

In (4.9) the hat-operator denotes the test filter with, $\hat{\Delta} \geq \Delta$. The correlation coefficient with the real SGS stress is higher for the scale similarity model than for the Smagorinsky model (Liu et al. (1994)), and the model provides for physical backscatter of turbulent energy. However, the scale similarity model does not provide for enough dissipation and is usually used in an ad hoc combination with a Smagorinsky term, which provides for additional dissipation and stabilises the simulations. An example of such a mixed model is the dynamic mixed model proposed by Zang et al. (1993)

It is a straightforward process to extend the scale similarity model for the SGS passive scalar flux

$$q_i = \widehat{\tilde{u}_i\tilde{\theta}} - \hat{\tilde{u}}_i\hat{\tilde{\theta}} \tag{4.10}$$

For instance, Calmet and Magnaudet (1997) applied the dynamic mixed model proposed by Zang et al. (1993) to LES of mass transfer in a turbulent channel.

4.4. Approximate deconvolution model

The approximate deconvolution model, ADM, by Stolz and Adams (1999) belongs to the group of velocity estimation models. In the ADM, the full unfiltered velocity is estimated by an approximate defiltering operation

$$\begin{aligned} u_i &\approx u_i^* = Q_N \star \tilde{u}_i \\ Q_N &= \sum_{\nu=0}^{N} (I - G)^{\nu} \approx G^{-1} \end{aligned} \tag{4.11}$$

where the star operator denotes a convolution and Q_N is an N-order approximation of the inverse filter kernel G^{-1}. The SGS stress is then computed from the definition $\tau_{ij} = \widetilde{u_{ij}^* u_{ij}^*} - \widetilde{u^*}_{ij}\widetilde{u^*}_{ij}$. With $N = 0$, the ADM corresponds to the scale-similarity model.

Like the scale similarity model, the ADM does not dissipate an adequate amount of energy. In order to model the energy transfer from resolved scales to the SGS an additional relaxation term $-\chi(I - Q_N \star G) \star \tilde{u}$ is added to the right hand side of equation (2.2). This is equivalent to an explicit filtering of the resolved velocity field at each time step. The model coefficient, χ, can be determined by a dynamic approach. LES of turbulent channel flow has shown a significant improvement over results obtained with the dynamic Smagorinsky model.

4.5. Stochastic models

The SGS models described so far depend on the resolved quantities in a deterministic way. However, the nature of the smallest turbulent scales appears as partly random to the resolved scales. The real sub-grid scale stress tensor

contains stochastic noise that cannot be modelled by any deterministic sub-grid-scale model.

Stochastic sub-grid modelling has been treated by several authors. Leith (1990) supplemented the Smagorinsky model by random SGS stresses calculated as the rotation of a stochastic potential. Schumann (1995) also modelled the stochastic behaviour of the SGS scales by adding random SGS stresses to the Smagorinsky model. Alvelius and Johansson (1999) proposed a stochastic model consisting of a modified Smagorinsky constant

$$C_s'^2 = C_s^2(1 + X) \tag{4.12}$$

where X is a stochastic process with prescribed variance and timescale. Stochastic modelling offers control of the magnitude and the time scale of the backscatter that could otherwise lead to numerical instabilities. See Chapter 5.1 for further details.

4.6. Transport equation models

Reynolds stress models including transport equations are frequent in RANS. They account for history effects and are able to accurately predict complex flows of interest in engineering applications. The same approach can be adopted to LES. In analogy with Reynolds decomposition, the full unfiltered velocity can be decomposed as

$$u_i = \tilde{u}_i + u_i^{'} \tag{4.13}$$

where $u_i^{'}$ is the fluctuating SGS velocity. If (4.13) is inserted into the definition of the SGS stress we have

$$\begin{aligned} \tau_{ij} &= L_{ij} + C_{ij} + R_{ij} \\ L_{ij} &= \widetilde{\tilde{u}_i\tilde{u}_j} - \tilde{u}_i\tilde{u}_j \\ C_{ij} &= \widetilde{\tilde{u}_i u_j^{'}} + \widetilde{\tilde{u}_j u_i^{'}} \\ R_{ij} &= \widetilde{u_i^{'} u_j^{'}} \end{aligned} \tag{4.14}$$

where L_{ij} is the Leonard stress, C_{ij} is the cross stress, and R_{ij} is the SGS Reynolds stress. Transport equations can be derived for either the complete SGS stress, or for some of the component parts. For example, Chaouat and Schiestel (2005) developed a three-equation SGS model based on the transport equations for the SGS Reynolds stress, the SGS kinetic energy, and the dissipation rate of the SGS Reynolds stress. Their model accurately describes the anisotropy of the turbulence field and it captures transition phenomena.

In Paper 2 we present a model based on a modelled transport equation for the complete SGS flux, see Chapter 5.2

CHAPTER 5

Summary of Papers

The performance of the new SGS models presented in Paper 1 and Paper 2 were tested in rotating homogeneous shear flow, which is an excellent case for developing and testing subgrid scale models. The simple geometry of the flow enables the use of the accurate spectral methods which makes it easy to separate SGS model features from the numerical errors. At the same time,

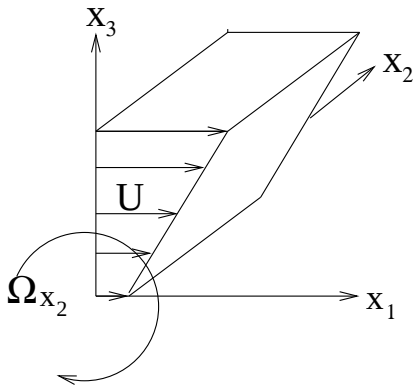

FIGURE 5.1. *Mean velocity profile and coordinate system. The frame rotates along the x_2-axis.*

the complication of a mean shear and and system rotation makes the flow physically interesting. The geometry of rotating homogeneous shear flow is illustrated in figure 5.1. U_1 is the only non zero mean velocity component and there is an imposed constant mean velocity gradient directed in the x_3-direction, $S_i = S\delta_{i3}$. The frame rotates along the x_2-axis at the angular velocity Ω. A constant mean scalar gradient can imposed in any direction.

5.1. Paper 1

In Paper 1, the stochastic model by Alvelius and Johansson is extended to a SGS scalar flux model. The stochastic model provides for backscatter of both kinetic energy and scalar variance, as can be seen from figure 5.2, and it predicts more realistic fluctuations at the smallest resolved scales compared to the

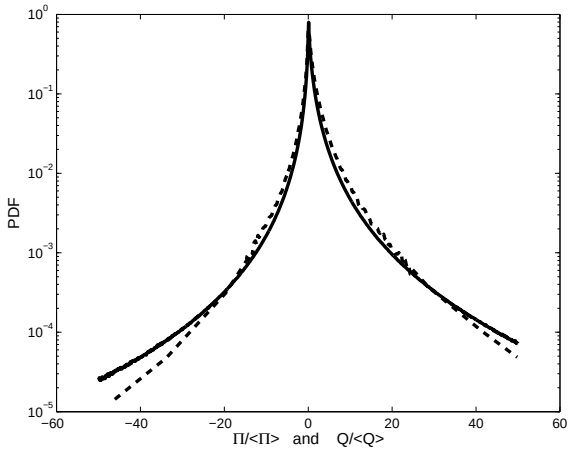

FIGURE 5.2. *PDF of the subgrid energy dissipation, dashed line, and scalar variance dissipation, solid line, according to the stochastic Smagorinsky model.*

Smagorinsky model. The time scale of the stochastic process is adjustable and it is concluded that backscatter represented by locally negative eddy viscosity does not cause numerical instability as long as it only occurs during short periods of time.

5.2. Paper 2

In Paper 2 a new explicit SGS scalar flux model is developed using the same kind of methodology that leads to the explicit algebraic scalar flux model, EASFM, developed by Wikström et al. (2000) for RANS. The new model is based on a modelled transport equation in which the unknown terms are modelled in the same way as in the EASFM, but with filtered quantities instead of Reynolds averaged quantities. In analogy with the EASFM, an equilibrium assumption is imposed in order to obtain an explicit model. The resulting model can be written as a mixed model including an eddy diffusion type of term, and the model includes information about both the resolved rate of strain, S_{ij}, and rotation rate tensors.

The new explicit model is validated in rotating homogeneous shear flow with an imposed constant passive scalar gradient. The new model responds to rotation in a more realistic way than the eddy diffusion model. For example, the direction of the mean SGS scalar flux predicted by the new model depends strongly on the rotation number with a significant subgrid flux component in the streamwise direction at the rotation numbers $R = 0$ and at $R = -1/2$, whereas the eddy diffusion model predicts a direction which is almost aligned

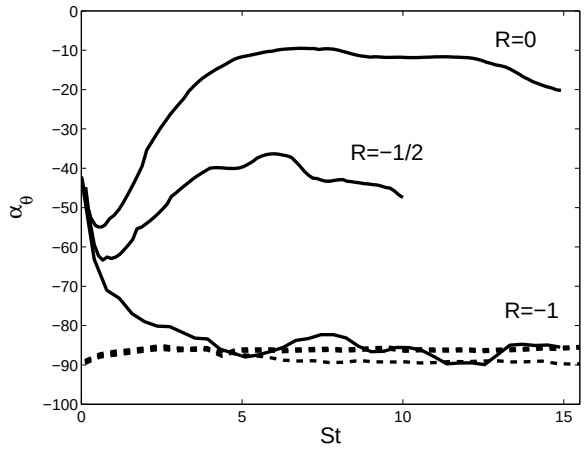

FIGURE 5.3. *The direction in degrees of the mean SGS scalar flux at three different rotation numbers. New model, solid line; eddy diffusion model, dashed line.*

with the transverse direction and does not depend to a significant degree on the system rotation, see figure 5.3. The new explicit model also provides for a better description of the magnitude and anisotropy of the mean scalar variance dissipation compared to the eddy diffusion model and the mixed similarity model.

5.3. Paper 3

In Paper 3, we describe a code for large eddy simulations of homogeneous shear flow with a constant mean passive scalar gradient. The use of periodic boundary conditions requires a transformation to a frame that moves with the mean flow. The code uses a pseudo-spectral technique. All spatial derivatives are accurately calculated in Fourier space, while the nonlinear terms are calculated in physical space. The aliasing errors that arise from the computation of the nonlinear terms are removed using a combination of truncation and phase shifts. The time advancement is performed in Fourier space using a third-order low storage Runge-Kutta method.

References

Ahlman D, Brethouwer G, Johansson A. 2006. Implementation of a method for simulation of compressible wall-bounded mixing flows. Tech. Rep.. Dept. of Mechanics, Royal Institute of Technology.

Piomelii U, Cabot W, Moin P, Lee S. 1991. Subgrid-scale backscatter in turbulent and transitional flows. *Phys. Fluids A* **3**, 1766-1771.

Smagorinsky J S. 1962. General circulation experiments with the primitive equations: I. The basic experiments. *Mon. Weather Rev.* **91**, 99.

Pope S. 2000. Turbulent flows. Cambridge University Press, Cambridge, UK.

Liu S, Meneveau C, Katz J, 1994. On the properties of similarity subgrid-scale models as deduced from measurements in a turbulent jet. *J. Fluid Mech.* **275**, 83-119.

Germano M, Piomelli U, Moin P, Cabot W. 1991. A dynamic subgrid-scale eddy viscosity model. *Phys. Fluids A* **3**, 1760-1765.

Lilly S. 1992. A proposed modification of the Germano subgrid scale closure method. *Phys. Fluids A* **4**, 633-635.

Chaouat B, Schiestel R, (2005) A new partially integrated transport equation model for subgrid-scale stresses and dissipation rate for turbulent developing flows. *Phys. Fluids* **17**, 035106.

Wang B, Bergstrom D (2005) A dynamic nonlinear subgrid-scale stress model. *Phys. Fluids*, **17**, 035109.

Bardina J Ferzinger J.H Reynolds, W.C. 1983. Improved turbulence models based on large eddy simulation of homogeneous incompressible flows. Technical report No. **TF-19** Stanford University

Stolz S, Adams N. 1999. An approximate deconvolution procedure for large-eddy simulation. *Phys. Fluids* **11**, 1699-1701.

Alvelius K, Johansson A V. 1999. Stochastic modelling in LES of a tubulent channel flow with and without system rotation. *In Doctoral Thesis*, Department of Mechanics KTH Sweden.

Schumann U. 1995. Stochastic backscatter of turbulence energies and scalar variance by random subgrid-scale fluxes. *Proceedings of the Royal Society of London, Series A, Phys.* **451**, 293-318.

Leith C E. 1990. Stochastic backscatter in a subgrid-scale model: Plane shear mixing layer. *Phys. Fluids A* **2**, 297-299.

Brethouwer G, Matsuo Y. 2005. DNS of rotating homogeneous shear flow and scalar mixing. Proc. 4th Int. Symp. on Turbulence and Shear Flow Phenomena (TSFP4), Williamsburg, USA. Editors: J A C Humphrey et al.

Kang H S, Meneveau C. 2001. Passive scalar anisotropy in a heated turbulent wake, new observations and implications for large eddy simulations. *J. Fluid Mech.* **442**, 161-170.

Meneveau C, Lund T, Cabot W. 1996. A Lagrangian dynamic sub-grid scale model of turbulence. *J. Fluid Mech.* **319** , 353-385.

Cerutti S. , Meneveau, C. 1998. Intermittency and relative scaling of subgrid scale energy dissipation in isotropic turbulence. *Phys. Fluids* **10** , 928-937.

Zang Y, Street R, Koseff J. 1993. A dynamic subgrid-scale model and its application to turbulent recirculating flows. *Phys. Fluids A* **5**, 3186-3196.

Calmet I, Magnaudet J. 1997. Large-eddy simulations of high-Schmidt number mass transfer in a turbulent channel flow. *Phys. Fluids* **9**, 438-455.

Wikström P M, Wallin S, Johansson A V. 2000. Derivation and investigation of a new algebraic model for the passive scalar flux. *Phys. Fluids* **12**, 688-702.

Acknowledgements

I would like to thank my supervisors Arne Johansson and Geert Brethouwer for guiding me in the LES-jungle and Dr. Stefan Wallin for his valuable comments on Paper 2.

I gratefully acknowledge the financial support from The Swedish Research Council.

1

Paper 1

Stochastic SGS modelling in rotating homogeneous shear flow with a passive scalar

By Linus Marstorp, Geert Brethouwer & Arne V. Johansson

A new stochastic Smagorinsky model for the subgrid stress and subgrid scalar flux is proposed. The new model is applied in LES of rotating homogeneous shear flow, which is an excellent case for developing and testing subgrid scale models. The proposed model provides for backscatter of kinetic energy and scalar variance, reduces the length scale of the subgrid dissipation, and reduces the time scale of the smallest resolved scales compared to the standard Smagorinsky model. At the same time, the flatness factor of the subgrid dissipation obtained from the stochastic model is of the same order of magnitude as for the Smagorinsky model.

---

1. Introduction

Accurate descriptions of turbulent flows including passive scalar mixing are desirable in many engineering applications and geophysical situations. A passive scalar is mixed by the flow field, but it has no effect on the flow. It can represent, for example, a pollutant carried by the flow or small temperature fluctuations.

A Large Eddy Simulation, LES, is an under-resolved numeric simulation of the Navier Stokes equation in which the influence of the unresolved, subgrid scales on the large scales has to be modelled. Many approaches to develop subgrid models in LES have been proposed, and many of them rely upon some kind of scale similarity assumption and depend on the resolved scales in a deterministic way. The widely known Smagorinsky model for the unclosed subgrid stress is based on a mixing length hypothesis where a SGS velocity scale is constructed from the resolved rate of strain and the filter length scale (Meneveau (2000)). It has several known drawbacks. Two examples are that it does not provide for backscatter of turbulent kinetic energy and that it over-predicts the correlation time of the resolved turbulence as pointed out by He (2002). The dynamic model, due to Germano et al (1991), provides for backscatter but the model constant yields too large fluctuations and it can easily become unstable. Applying averaging in homogeneous directions to obtain the constant eliminates the stability problem but the model looses generality and the ability to

account for backscatter. In the similarity model developed by Bardina et al. (1983) the full unfiltered velocity field is estimated by the resolved velocity and the SGS stress is computed by a secondary explicit filtering at equal or larger filter scale. The model does not provide for enough dissipation and is usually used in an ad hoc combination with a Smagorinsky term. A recent SGS model by Stolz and Adams (1999) is the approximate deconvolution model, ADM, which can be regarded as a generalised similarity model. Deterministic models based on scale similarity have proved to perform well in many situations. However, the nature of the smallest turbulent scales appears as partly random to the resolved scales, and the real subgrid scale stress tensor extracted from DNS contains stochastic noise that cannot be modelled by any deterministic subgrid-scale model. De Stefano et al. (2005) applied a wavelet denoising technique to isotropic turbulence to separate the incoherent part (close to white noise) from the coherent part of the velocity field. They found a very large amount of incoherent noise in the subgrid stress tensor. We believe that this stochastic influence of the subgrid scales on the resolved scales has to be modelled in order to get a correct description of the smallest resolved scales. In this paper we will use a stochastic process to model the stochastic influence of the SGS scales.

The use of stochastic processes in subgrid modelling in LES has been treated by Leith (1990), Schumann (1995), and Alvelius and Johansson (1999). Leith supplemented the Smagorinsky model by random SGS stresses calculated as the rotation of a stochastic potential. Schumann also based his model on the Smagorinsky model and added the stochastic behaviour of the SGS scales by random SGS stresses for the velocity field, and by random SGS scalar fluxes for the passive scalar field. Both Leith and Schumann focused on how to obtain a correct description of the stochastic backscatter. Alvelius and Johansson (1999) showed that the Smagorinsky model predicts a too large length scale of the subgrid dissipation and proposed a new stochastic model that solved this problem. The purpose of this study is to follow the approach of Alvelius and Johansson to develop a new stochastic model for the subgrid scales of the velocity field and validate this new model. At the same time, we apply the idea of stochastic modelling to the subgrid scales of a passive scalar field.

2. Stochastic subgrid modelling

2.1. *Filtered equations*

The filtered incompressible Navier-Stokes and passive scalar equations in a rotating frame read (ϵ_{ijk} is the permutation tensor)

$$\begin{aligned}
&\frac{\partial \tilde{u}_i}{\partial t} + \tilde{u}_j \frac{\partial \tilde{u}_i}{\partial x_j} = -\frac{1}{\rho}\frac{\partial \tilde{p}}{\partial x_i} + \nu \nabla^2 \tilde{u}_i - 2\epsilon_{ijk}\Omega_j \tilde{u}_k - \frac{\partial \tau_{ij}}{\partial x_j} \\
&\frac{\partial \tilde{u}_i}{\partial x_i} = 0 \\
&\frac{\partial \tilde{\theta}}{\partial t} + \tilde{u}_j \frac{\partial \tilde{\theta}}{\partial x_j} = \frac{\nu}{Pr}\nabla^2 \tilde{\theta} - \frac{\partial q_j}{\partial x_j}
\end{aligned} \tag{1}$$

where $\tilde{u}_i$ and $\tilde{\theta}$ denote the filtered velocity and passive scalar respectively, and where $\tilde{p}$ includes both the pressure and the centrifugal force. Ω_i is the system rotation vector and Pr is the Prandtl number. The subgrid scalar stress tensor $\tau_{ij} = \widetilde{u_i u_j} - \tilde{u}_i \tilde{u}_j$ and the subgrid flux vector $q_j = \widetilde{\theta u_j} - \tilde{\theta}\tilde{u}_j$ have to be modelled in order to close the equations.

2.2. *A stochastic model*

The idea behind the present stochastic subgrid model is to model the random behaviour of the subgrid stress and flux by a stochastic process, which can improve the description of the smallest resolved scales. The new stochastic model is based on the Smagorinsky model for the unclosed subgrid-scale stress tensor, τ_{ij}, and subgrid-scale flux, q_j, which read

$$\begin{aligned}
\tau_{ij} &= -2\nu_T \tilde{S}_{ij} \\
q_j &= -\frac{\nu_T}{Pr_T}\frac{\partial \tilde{\theta}}{\partial x_j}
\end{aligned} \tag{2}$$

where the turbulent Prandtl number, Pr_T, is a constant and $\nu_T = (C_s\Delta)^2|\tilde{S}_{ij}|$ is the eddy viscosity. C_s is the Smagorinsky constant, Δ is the filter width, and $\tilde{S}_{ij}$ denotes the filtered, or resolved, rate of strain. Similar to Alvelius and Johansson (1999), we model the eddy viscosity as a sum of the Smagorinsky model and a stochastic term

$$\nu_T = C_s^2(1 + X(x,t))\Delta^2|\tilde{S}_{ij}| \tag{3}$$

The part corresponding to the Smagorinsky model generates the right amount of mean dissipation whereas the stochastic part creates realistic SGS fluctuations. $X(x,t)$ are independent processes obeying the Ornstein-Uhlebeck equation at each spatial point

$$dX(x,t) = aX(x,t)dt + b\sqrt{2a}dW(x) \tag{4}$$

where a and b are constants and $dW(x)$ are spatially independent random numbers with the normal distribution $N(0, \sqrt{dt})$. The solution $X(x,t)$ to (4) is a

stationary process with zero mean, $E[X(x_0,t)] = 0$, and constant variance, $V[X(x_0,t)] = b^2$. The time scale of the process can be characterised by the decay rate of the correlation $E[X(x_0,t)X(x_0,t_0+t)]/V_X = exp(-at)$. It follows that the time scale of the process,$\tau_X = 1/a$, decreases with increasing values of a.

The time scale of the stochastic noise that we intend to model is that of the subgrid scale velocity field, and since the SGS field is advected by the resolved scales the time scale $\tau_X = 1/a$ should naturally be computed in a Lagrangian frame of reference. This is, however, beyond the scope of this study. Instead, the length scale, Δ, of the subgrid field is used to estimate an Eulerian time scale of the subgrid scales. From dimensional arguments we have

$$\tau_X = C\left(\Delta^2/\langle\Pi\rangle\right)^{1/3} \tag{5}$$

where C is a constant of order 1 and Π is the subgrid dissipation of resolved kinetic energy

$$\Pi = -\tau_{ij}\tilde{S}_{ij} \tag{6}$$

Since $\tau_X = 1/a$ this defines a. Hence, stochastic noise which has a correlation time about as long as the time scale of the subgrid velocity field and which is uncorrelated in space, enters the subgrid stress through the eddy viscosity. The eddy diffusivity for the subgrid scalar flux is modelled by (2) using a constant $Pr_T = 0.6$ and thus contains also stochastic noise.

3. Simulations

The performance of the new model was tested in rotating homogeneous shear flow, which is an excellent case for developing and testing subgrid scale models. The simple geometry of the flow enables the use of the accurate spectral methods which makes it easy to separate SGS model features from the numerical errors. At the same time the complication of a mean shear and and system rotation makes the flow physically interesting.

The filtered incompressible Navier-Stokes equations with a constant uniform shear, $U_i = Sx_3\delta_{i1}$, and the passive scalar equation with a mean scalar gradient, $G_i = \delta_{i3}$, were solved using a pseudo spectral code with a third order Runge-Kutta method for time advancement. Rogallo's method has been used to simulate homogeneous shear flow, i.e. the grid moves along with the mean flow to enable the use of periodic boundary conditions, and it is re-meshed periodically. Some information is lost during the re-meshing. However, the losses are not significant for the evolution of the flow. LES with 128^3, 64^3 and 32^3 grid-points were performed in a periodic box with the dimensions $4\pi \times 3\pi \times 2\pi$ with three different subgrid models; the standard Smagorinsky model, the dynamic model as defined by Lilly (1992) (both with model constant averaging in all homogeneous directions and with clipping of large negative values), and the

new stochastic model described above. The model parameter b was adjusted to fit with the amount of modelled backscatter with observations from filtered DNS data. Two different values $C = 0.2$ and $C = 0.8$ were examined.

Fully developed turbulence obtained from isotropic decay was used as initial condition and the flow is rotating about the spanwise direction, $\Omega_i = \Omega\delta_{i2}$, at the non-dimensional rotation numbers $R = 2\Omega/S = 0$, $-1/2$, and -1. The initial scalar field was without any fluctuations. The initial non-dimensional shear rate was chosen as $S\tilde{K}/\tilde{\epsilon} = 3.38$, and the initial turbulence Reynolds number was $Re_T = \tilde{K}^2/(\tilde{\epsilon}\nu) = 1500$.

The LES results were compared to DNS data of homogeneous turbulent shear flow represented on $960 \times 512 \times 576$ grid-points in a box with the dimensions $4\pi \times 2\pi \times 2\pi$. The DNS data was filtered to the resolutions 32^3, 64^3 and 128^3 using the same Gaussian filter as Cerutti and Meneveau (1998). In the DNS the initial Reynolds number, $Re_T = 135$, is lower than in the LES. Moreover, the mean scalar gradient is directed in streamwise direction instead of the transverse direction. However, we believe that it is appropriate to compare data on the amount of backscatter with the LES results. We will also use the filtered data to compare the intermittency of the SGS energy dissipation to the intermittency of the SGS scalar variance dissipation.

4. Results

4.1. *Large scale statistics*

Figure 1 shows the time development of the turbulent kinetic energy. The flow is strongly destabilised at $R = -0.5$. At $R = -1$ $\tilde{K}$ still grows but at much slower rate than at $R = 0$. These observations agree well with Brethouwer and Matsuo (2005) and show that all models produce the right amount of mean dissipation. The growth has a pronounced exponential part, $\tilde{K} = \tilde{K}_0 e^{\alpha St}$ at $R = 0$ and $R = -1/2$. At $R = 0$ the exponential growth rate is in agreement with the experiment by Tavoularis and Corrsin (1981). $C_s = 0.10$ is used in the standard Smagorinsky and stochastic model, which is equal to the value $C_s \approx 0.10$ predicted by the dynamic model. This value is also close to the value $C_s = 0.11$ suggested by Canuto and Cheng (1997) for homogeneous shear flow, but much smaller than the value $C_s = 0.19$ used by Bardina et al. (1983). The time development of $\tilde{K}$ (and the Reynolds stresses) are very similar for the LES with the stochastic model and the dynamic model according to the figure. The results for the Smagorinsky model and stochastic model were in fact indistinguishable, as should be expected.

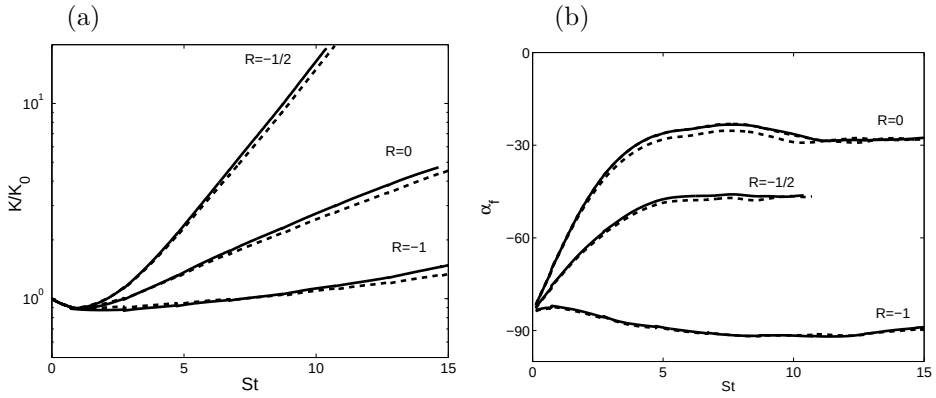

FIGURE 1. *(a): The time history of the turbulent kinetic energy. (b): The direction of turbulent scalar flux. Dynamic model, dashed line; stochastic and Smagorinsky model, solid line.*

Next, we turn our attention to the scalar mixing. The direction of the turbulent flux is defined as

$$\alpha_f = atan\left(\frac{\langle\tilde{\theta}'\tilde{u}_3'\rangle}{\langle\tilde{\theta}'\tilde{u}_1'\rangle}\right) \tag{7}$$

where $\tilde{u}_i'$ and $\tilde{\theta}'$ denote the fluctuating velocity and scalar components, and where $\langle\tilde{\theta}'\tilde{u}_1'\rangle$ and $\langle\tilde{\theta}'\tilde{u}_3'\rangle$ are the mean turbulent scalar fluxes in the x_1 and x_3 direction, respectively. In figure 1, the development of α_f is seen to depend on the rotation number. The angle α_f in the LES with the standard, dynamic, and stochastic Smagorinsky model approaches the same equilibrium values and the results were found to yield good agreement with DNS results of Brethouwer and Matsuo and Rogers et al. (1989). Also here, the results of the stochastic model are very close to those of the Smagorinsky model. The ratio of the mean turbulent diffusivity to the molecular diffusivity is about 50 showing that the similarities between the predictions of the stochastic and the Smagorinsky model are not owing to low Reynolds number.

4.2. *Backscatter*

Despite the small differences in large scale statistics in the LES with the standard Smagorinsky and stochastic model, there are significant differences at the smaller scales. The subgrid dissipation of the stochastic model can be decomposed into two parts

$$\Pi = C_s^2\Delta^2|\tilde{S_{ij}}|^3 + XC_s^2\Delta^2|\tilde{S_{ij}}|^3 \equiv \Pi_S + \Pi_X \tag{8}$$

where Π_S is a standard Smagorinsky contribution to Π and where Π_X is a stochastic contribution which is linear in X. From the PDF of Π_X presented

in figure 2 we see that it is symmetric about its mean value $\langle \Pi_X \rangle = 0$ and that it allows the stochastic model to provide for backscatter if the variance of X is sufficiently large. Backscatter is local energy transfer from the SGS into the resolved scales, see Piomelii et al. (1991) and and Cerutti and Meneveau (1998). In the present model backscatter is represented by intermittently negative eddy viscosity. This is of course only a very simple model for the real backscatter phenomenon, assuming that the SGS stress is aligned with the resolved rate of strain. Π_S has no backscatter of turbulent kinetic energy and has a positive mean value. The combination of the Smagorinsky model and the stochastic term thus accounts for a combination of mean forward energy flux and backscatter.

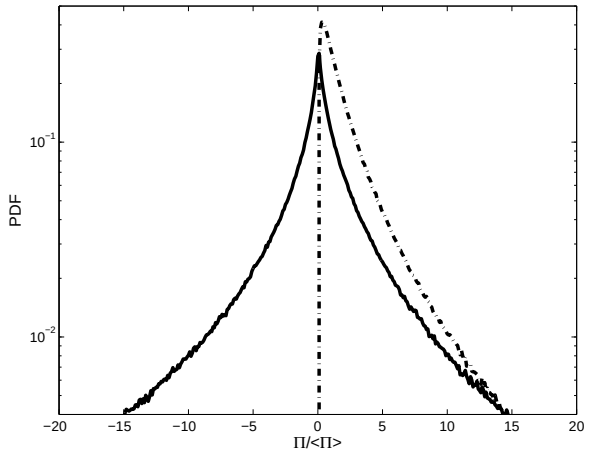

FIGURE 2. *PDF of the subgrid dissipation according to the stochastic model.* Π_X, *solid line;* Π_s, *dash-dotted line*

If we assume that it is appropriate to model all backscatter by the stochastic eddy viscosity, we can adjust the parameter b so that the real and modelled amount of backscatter matches observations. Piomelii et al. (1991) found that the probability of backscatter is about 50% in turbulent channel flow. The present stochastic model is not able to predict such large probability unless $b \to \infty$. Instead, we follow the approach of Wang and Bergstrom (2005) and separate the the mean SGS dissipation into averaged forward- $\langle \Pi^+ \rangle$ and backscatter $\langle \Pi^- \rangle$ contributions

$$\langle \Pi^+ \rangle + \langle \Pi^- \rangle = \langle \Pi \rangle \tag{9}$$

In the filtered DNS data the ratio $-\langle \Pi^- \rangle / \langle \Pi^+ \rangle$ is typically 0.4 and it increases somewhat at smaller filter scales. A constant b in the stochastic model

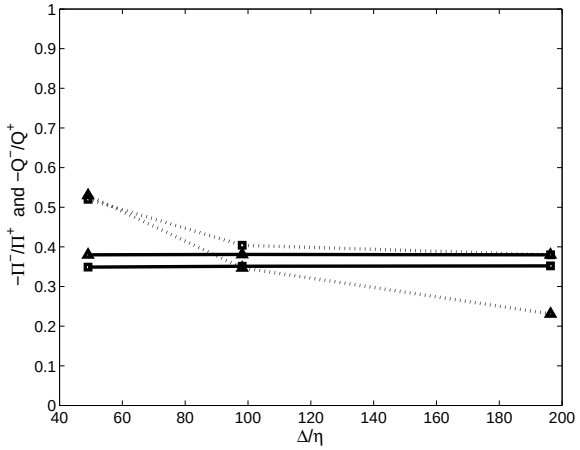

FIGURE 3. *Amount of backscatter. Stochastic model, solid lines; DNS data, dotted lines. Energy backscatter, square; Scalar backscatter, triangle.*

implies a constant ratio $-\langle\Pi^-\rangle/\langle\Pi^+\rangle$. We choose $b = 2.3$ which implies $-\langle\Pi^-\rangle/\langle\Pi^+\rangle \approx 0.4$, which yielded a fair overall agreement with the DNS results as shown in figure 3. The rotation number does not have a significant impact on the amount of backscatter in the LES. The model parameter a does not affect the probability for backscatter and has only a very small impact on the averaged backscatter due to the response of the flow field.

The stochastic model accounts also for backscatter of scalar variance in the same manner as for the turbulent kinetic energy. This is shown in figure 4, where the PDF of the total scalar variance dissipation,

$$Q = -2q_i\partial\tilde{\theta}'/\partial x_i \tag{10}$$

is plotted together with the PDF of the total SGS dissipation, for the LES with a resolution of 128^3. In agreement with the DNS data in figure 4, the peak of scalar PDF is more narrow than for the velocity field indicating that the scalar field is more intermittent than the velocity field. The amount of scalar variance backscatter $-\langle Q^-\rangle/\langle Q^+\rangle$ in figure 3, agrees reasonably well with that of the DNS data despite the fact that we calibrated the constant b to fit the data on the velocity field. It seems appropriate to use the same process X and parameter b as for the velocity field.

Negative eddy viscosity has to be treated with care. The stochastic model predicts locally negative total viscosity $(\nu_T + \nu)$ and can be unstable under some

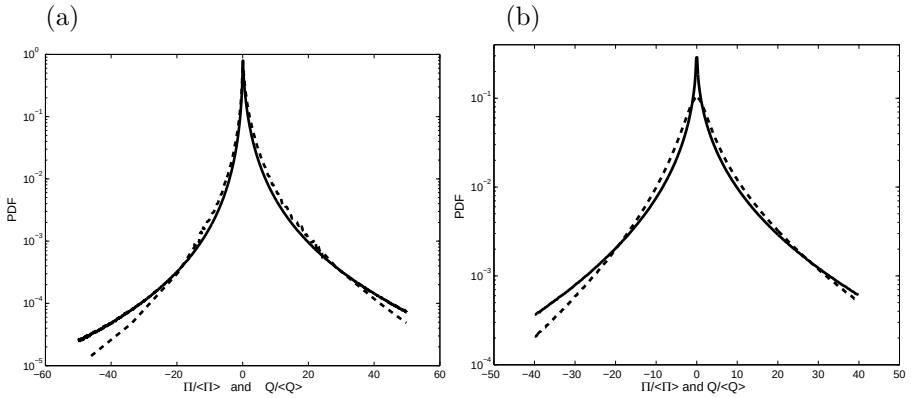

FIGURE 4. *PDF of the energy SGS dissipation and the scalar variance SGS dissipation according to (a): the stochastic Smagorinsky model (b): the filtered DNS data. Energy SGS dissipation, dashed line; scalar variance SGS dissipation, solid line.*

circumstances. A large time scale, τ_X, and a large variance of the stochastic process increases the probability for numerical instability. For the present choice of parameters and initial conditions it was *not* necessary to clip negative values of subgrid dissipation because of the short time scale of the backscatter. Locally negative total viscosity is not dangerous as long as it only occurs during short periods of time.

4.3. *Intermittency of SGS dissipation*

The flatness factor of the subgrid dissipation

$$F = \frac{\langle (\Pi - \langle \Pi \rangle)^4 \rangle}{\langle (\Pi - \langle \Pi \rangle)^2 \rangle^2} \tag{11}$$

is a measure of the intermittency. Large values indicate high intermittency. Cerutti and Meneveau (1998) compared the flatness factor of the subgrid dissipation predicted by various subgrid stress models using a velocity field obtained from DNS. They found that the dynamic model without spatial averaging predicts a too intermittent SGS dissipation and that the Smagorinsky model predicts SGS dissipation that is about as intermittent as the real SGS dissipation. The flatness factor of Π, at $R = 0$ according to the LES with the stochastic model, the clipped dynamic model ($C_s^2 > -0.01$) and the standard Smagorinsky model are plotted in figure 5. The constant a in the stochastic model is varied by changing C in (5). We can see that the flatness predicted by the

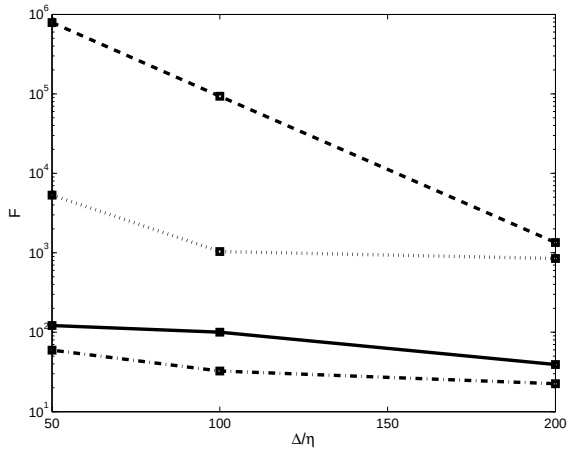

FIGURE 5. *The flatness of the subgrid dissipation. Clipped dynamic model, dashed line; stochastic model with C=0.8, dotted line; stochastic model with C=0.2, solid line; standard Smagorinsky model, dash-dotted line.*

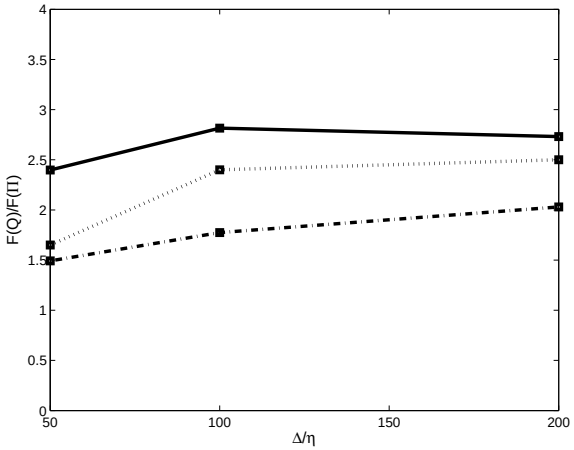

FIGURE 6. $F(Q)/F(\Pi)$. *Stochastic model, solid line; standard Smagorinsky model, dash-dotted line; filtered DNS, dotted line.*

stochastic model with $C = 0.2$ is of the same order of magnitude as for the standard Smagorinsky model, whereas the intermittency of Π according to the clipped dynamic model and the stochastic model with $C = 0.8$ is much too large. Hence, by choosing $C = 0.2$ the stochastic Smagorinsky model provides for backscatter in the form of negative viscosity without being too intermittent.

Both the dynamic model and the stochastic model allow locally negative total viscosity. We believe that the reason why the result of the dynamic model is more intermittent is the time scale of the backscatter rather than the negative viscosity itself.

The PDF of Π and Q in section 4.2 indicated that Q is more intermittent than Π. From figure 6 we see that this is the case. According to the filtered DNS data the ratio of the flatness factor of Q to that of Π varies from 2.5 to 1.6 within the present range of filter scales. The ratio predicted by the Smagorinsky model is somewhat smaller and the result of the stochastic model is slightly larger.

4.4. *Correlation time*

Time correlations are important in LES of sound generation, see He (2002). He (2002) showed that in LES with the Smagorinsky model the time scales are overpredicted at all turbulent length scales, especially close to the filter scale. They suggested a stochastic force to solve the problem. The present stochastic model adds such a stochastic SGS force to the velocity field. We have chosen to study the time correlations in decaying isotropic turbulence. The results of the correlation time scales are then affected by the decay of the turbulence intensity, but it is appropriate for comparison of different SGS models since the mean turbulent kinetic energy develop in the same way for both the Smagorinsky and the stochastic model. We follow the steps of He et al. and define the correlation coefficients as

$$c(k,t,\tau) = \frac{\langle u_i(k,t)u_i(-k,t+\tau)\rangle}{\langle u_i(k,t)u_i(-k,t)\rangle} \tag{12}$$

where the average operator denotes averaging in a spherical shell in wave number space. In figure 7 the time correlation coefficients at $k = 0.75k_c$ of the present stochastic model are seen to decay faster in time compared to the Smagorinsky model. In the case $C = 0.2$ the correlation coefficient is seen to decrease faster than at $C = 0.8$. This is correct since the time scale of X is smaller at $C = 0.2$. The correlation time scale as a function of k is computed as

$$\tau^*(k) = \int_0^\infty c(k,t_1,\tau)d\tau \tag{13}$$

and is shown in figure 8. The stochastic model predicts shorter correlation times than the Smagorinsky model for all k, but in particular at large k the reduction of τ^* is large. This is where it is most needed according to He et al.

4.5. *Subgrid dissipation length scale*

We study the length scale of the subgrid dissipation at the most destabilised rotation number $R = -1/2$ where resolved length scales grow very fast. The

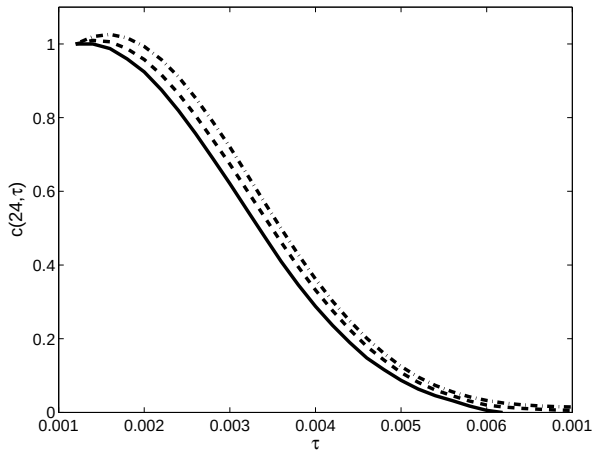

FIGURE 7. *The time correlation coefficient for* $k = 0.75k_c$. *Standard Smagorinsky model, dash-dotted line ; Stochastic model* $C = 0.8$, *dashed line;* $C = 0.2$, *solid line.*

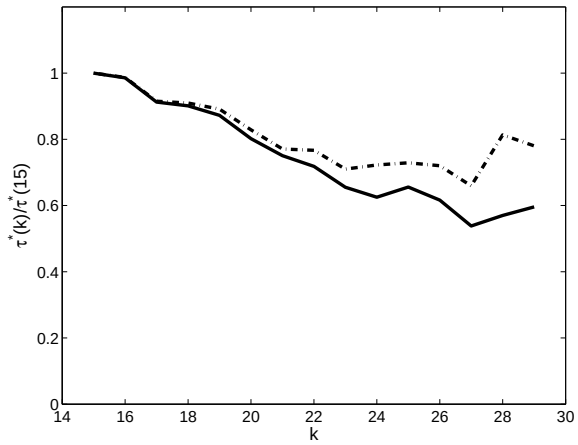

FIGURE 8. *Time scale,* $\tau^*(k)$, *as a function of the wavenumber. Standard Smagorinsky model, dash-dotted line ; Stochastic model with* $C = 0.2$, *solid line.*

length scale of the subgrid dissipation is computed from the correlation

$$L_\Pi = \int_0^{l_x} \frac{\langle \Pi'(x_0), \Pi'(x_0 + x) \rangle}{\langle \Pi'^2 \rangle} dx \tag{14}$$

where l_x is half of the box length in the the streamwise direction, and $\Pi' = \Pi - \langle\Pi\rangle$ is the fluctuating part of the subgrid dissipation. According to the DNS of channel flow by Alvelius and Johansson (1999) the Smagorinsky model overpredicts L_Π, and they found the length scale of the real SGS dissipation to be smaller than the streamwise grid size everywhere in the channel. The

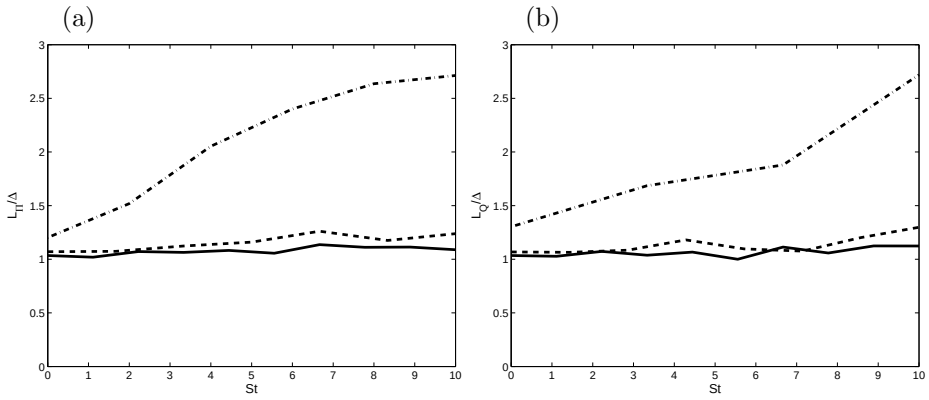

FIGURE 9. *The time development of the length scale of (a): the subgrid dissipation (b): the scalar variance subgrid dissipation. Stochastic model, solid line; standard Smagorinsky model, dash-dotted line; dynamic model, dashed line.*

LES-results presented in figure 9 show that the Smagorinsky model predicts a length scale that becomes significantly larger than the filter-scale whereas the stochastic model keeps L_Π at the size of the filter scale throughout the whole simulation if $b = 2.3$ and $C = 0.2$. The clipped dynamic model ($C_s^2 > -0.01$) also reduces L_Π and keeps it at the size of the filter scale, but the model is potentially unstable. The reduction of streamwise integral lengthscale of the scalar variance dissipation is similar as for the energy dissipation according to figure 9.

5. Conclusions

LES of rotating homogeneous shear flow with a passive scalar was performed. Three different subgrid models were used: the standard Smagorinsky model, the dynamic Smagorinsky model and a newly developed stochastic model. The choice of subgrid model had a small influence on the large scale velocity and scalar statistics, but a large effect on the smaller scales. The proposed stochastic Smagorinsky model was shown to reduce the time scale of the smallest resolved scales, to reduce the length scale of the subgrid energy and scalar variance dissipation and to provide for significant backscatter. This may be a promising feature for the development of improved subgrid scale models for

aeroacoustics and for reacting flows, where the properties of the subgrid scales are very important. The LES with the dynamical model using spatial averaging did not provide for backscatter. With clipping of large negative values of the dynamic model constant instead of spatial averaging the dynamic model accounts for backscatter, but due to long correlation time of the negative eddy viscosity the intermittency of the dissipation was very high and numerical instabilities occurred. The time scale of the backscatter predicted by the proposed model is adjustable. For the suggested model parameters the intermittency of the subgrid dissipation was of the same order of magnitude as for the standard Smagorinsky model and realistic. Locally negative eddy viscosity is not dangerous as long as it only occurs during short periods of time.

References

Alvelius K, Johansson A V. 1999. Stochastic modelling in LES of a tubulent channel flow with and without system rotation. *In Doctoral Thesis*, Department of Mechanics KTH Sweden.

Bardina J Ferzinger J.H Reynolds, W.C. 1983. Improved turbulence models based on large eddy simulation of homogeneous incompressible flows. Technical report No. **TF-19** Stanford University.

Brethouwer G. 2005. The effect of rotation on rapidly sheared homogeneous turbulence and passive scalar transport. Linear theory and direct numerical simulations, J. Fluid Mech. **542**, 305- 342.

Brethouwer G, Matsuo Y. 2005. DNS of rotating homogeneous shear flow and scalar mixing. Proc. 4th Int. Symp. on Turbulence and Shear Flow Phenomena (TSFP4), Williamsburg, USA. Editors: J A C Humphrey et al.

Canuto V M, Cheng Y. 1997. Determination of the Smagorinsky-Lilly constant C_s *Phys. Fluids* **9**, 1368-1378.

Cerutti S, Meneveau C. 1998. Intermittency and relative scaling of subgrid-scale energy dissipation in isotropic turbulence. *Phys. Fluids* **10**, 928-937.

Germano M, Piomelli U, Moin P, Cabot W. 1991. A dynamic subgrid-scale eddy viscosity model. *Phys. of Fluids A* **3**, 1760-1765.

He G, Rubinstein R, Wang L. 2002. Effects of subgrid-scale modeling on time correlations in large eddy simulation. *Phys. Fluids* **14**, 2186-2193.

Leith C E. 1990. Stochastic backscatter in a subgrid-scale model: Plane shear mixing layer. Phys. of Fluids A **2**, 297-299.

Lilly S. 1992. A proposed modification of the Germano subgrid scale closure method. *Phys. Fluids A* **4**, 633-635.

Meneveau C. 2000. Scale-Invariance and Turbulence Models for Large-Eddy Simulation. *Ann. rev. fluid mech.* **32**, 1-32.

Piomelii U, Cabot W, Moin P, Lee S. 1991. Subgrid-scale backscatter in turbulent and transitional flows. *Phys. Fluids A* **3**, 1766-1771.

Rogers M M, Mansour N N, Reynolds W C. 1989. An algebraic model for the turbulent flux of a passive scalar. *J. Fluid Mech.* **203**, 77-101.

Schumann U. 1995. Stochastic backscatter of turbulence energies and scalar variance by random subgrid-scale fluxes. *Proceedings of the Royal Society of London, Series A, Phys.* **451**, 293-318.

De Stefano G, Goldstein D, Vasilyev O. 2005. On the role of subgrid-scale coherent modes in large-eddy simulation. *J. Fluid Mech.* **525**, 263-274.

Stolz S, Adams N. 1999. An approximate deconvolution procedure for large-eddy simulation. *Phys. Fluids* **11**, 1699-1701.

Tavoularis S, Corrsin S. 1981. Experiments in nearly homogeneous turbulent shear flow with a uniform mean temperature gradient. Part 2. The fine structure, *J. Fluid Mech.* **104**, 349 - 367.

Wang B, Bergstrom D. 2005. A dynamic nonlinear subgrid-scale stress model. *Phys. Fluids* **17**, 035109.

2

Paper 2

A new model for the subgrid passive scalar flux

By Linus Marstorp, Geert Brethouwer & Arne V. Johansson

A new subgrid scalar flux model based on a modelled transport equation for the subgrid scalar flux is proposed and validated in rotating homogeneous shear flow. The new subgrid scalar flux model is derived using the same kind of methodology that leads to the EASFM of Wikström et al. (2000). It predicts the magnitude and the anisotropy of the scalar variance SGS dissipation in a more realistic way than the eddy diffusion model and the mixed similarity model.

---

1. Introduction

Passive scalar mixing in turbulent flows can be observed in industrial applications and in our environment. A passive scalar is mixed by the flow, but it has no effect on the flow. It can represent, for example, a pollutant carried by the flow or small temperature fluctuations. Knowledge of passive scalar mixing is also a first step towards the understanding of reactive flows where the mixing of species plays an important role. Large Eddy Simulations (LES) is a promising tool to predict mixing of scalars in turbulent flows. It has a good ability to calculate turbulent scalar transport in rotating flows as shown by Marstorp et al. (2005) whereas this is difficult for other scalar transport models.

In LES, the eddy diffusion model is a widely used model for the subgrid scalar field. It is simple and computationally cheap, but it has several known drawbacks. One example is its inability to predict the anisotropy of the subgrid passive scalar field, as pointed out by Kang and Meneveau (2001). They showed that the anisotropy of the mean scalar variance SGS dissipation predicted by the eddy diffusion model is approximately the same as that for the mean squared scalar gradient. This is not appropriate since the anisotropy of the mean squared gradient is not in general the same as that of the mean SGS dissipation. The mixed scale similarity model due to Bardina et al. (1983) was originally a SGS model for the velocity field, but it has been extended to a SGS scalar flux model by several authors. For example, Calmet and Magnaudet (1997) applied the dynamic mixed model proposed by Zang et al. (1993) to LES of mass transfer in a turbulent channel. The scale similarity part of the mixed model accounts locally both for backward and forward flux of scalar variance but the eddy diffusivity part provides for most of the mean scalar

variance dissipation.

Recently Wikström et al. (2000) proposed an explicit algebraic scalar flux model, EASFM, based on a modelled transport equation for the Reynolds averaged scalar flux. It predicts the scalar flux more accurately in shear flows than the eddy diffusivity model, and it is computationally cheap. The objective of this study is to develop a new model for the subgrid scalar flux, by applying the same kind of methodology that leads to the EASFM for the Reynolds averaged scalar flux, and to test the new explicit SGS model in rotating homogeneous shear flow. The new explicit SGS model includes information about both the resolved rate of strain, S_{ij}, and rotation rate tensors and is expected to improve performance in rotating flows. At the same time the explicit form makes the new model about as computationally cheap as the eddy diffusion model.

2. Filtered equations

The filtered incompressible Navier-Stokes and passive scalar equations in a rotating frame reads (ϵ_{ijk} is the alternating tensor)

$$\begin{aligned}
&\frac{\partial \tilde{u}_i}{\partial t} + \tilde{u}_j \frac{\partial \tilde{u}_i}{\partial x_j} = -\frac{1}{\rho}\frac{\partial \tilde{p}}{\partial x_i} + \nu \nabla^2 \tilde{u}_i - 2\epsilon_{ijk}\Omega_j \tilde{u}_k - \frac{\partial \tau_{ij}}{\partial x_j} \\
&\frac{\partial \tilde{u}_i}{\partial x_i} = 0 \\
&\frac{\partial \tilde{\theta}}{\partial t} + \tilde{u}_j \frac{\partial \tilde{\theta}}{\partial x_j} = \frac{\nu}{Pr}\nabla^2 \tilde{\theta} - \frac{\partial q_j}{\partial x_j}
\end{aligned} \tag{1}$$

where $\tilde{u}_i$ and $\tilde{\theta}$ denotes the filtered velocity and passive scalar respectively, and where $\tilde{p}$ includes both the pressure and the centrifugal force. Ω_i is the system rotation vector, ν is the viscosity, and Pr is the Prandtl number. The SGS stress, $\tau_{ij} = \widetilde{u_i u_j} - u_i u_j$, and the SGS scalar flux, $q_i = \widetilde{u_i \theta} - \tilde{u}_i \tilde{\theta}$, have to be modelled in order to close the system of equations.

3. Proposed model

The new subgrid scalar flux model can be derived in the same manner as the EASFM of Wikström et al. (2000), but with filtered quantities instead of Reynolds averaged quantities. In a inertial frame of reference the subgrid flux obeys the transport equation

$$\frac{Dq_i}{Dt} = P_{i\theta}^{SGS} + D_{i\theta}^{SGS} + \Pi_{i\theta}^{SGS} - \epsilon_{i\theta}^{SGS} \tag{2}$$

where

$$P_{i\theta}^{SGS} = -q_j \frac{\partial \tilde{u}_i}{\partial x_j} - \tau_{ij}\frac{\partial \tilde{\theta}}{\partial x_j} \tag{3}$$

is the production of subgrid scalar flux from the resolved scales, and

$$\begin{aligned}\Pi_{i\theta}^{SGS} =& \frac{1}{\rho}\left(\widetilde{p\frac{\partial\theta}{\partial x_i}} - \tilde{p}\frac{\partial\tilde{\theta}}{\partial x_i}\right)\\ \epsilon_{i\theta}^{SGS} =& \left(\nu + \frac{\nu}{Pr}\right)\left(\widetilde{\frac{\partial\theta}{\partial x_j}\frac{\partial u_i}{\partial x_j}} - \frac{\partial\tilde{\theta}}{\partial x_j}\frac{\partial\tilde{u}_i}{\partial x_j}\right)\end{aligned} \tag{4}$$

are the subgrid pressure scalar-gradient correlation and subgrid scalar flux dissipation respectively. D_i includes both turbulent and molecular diffusion.

In analogy with the EASFM, we normalise the SGS scalar flux with the subgrid kinetic energy K^{SGS} and subgrid scalar intensity K_θ^{SGS}

$$\begin{aligned}\xi_i &= q_i/\sqrt{K^{SGS}K_\theta^{SGS}}\\ K^{SGS} &= \left(\widetilde{u_i u_i} - \tilde{u}_i\tilde{u}_i\right)/2\\ K_\theta^{SGS} &= \left(\widetilde{\theta\theta} - \tilde{\theta}\tilde{\theta}\right)/2\end{aligned} \tag{5}$$

The transport equation for the normalised SGS scalar flux, ξ_i, yields

$$\frac{D\xi_i}{Dt} - D_i^\xi = \frac{1}{2}\xi_i\left(\frac{P_\theta^{SGS} - \epsilon_\theta^{SGS}}{K_\theta^{SGS}} + \frac{P_K^{SGS} - \epsilon_K^{SGS}}{K_\theta^{SGS}}\right) + \frac{P_{i\theta}^{SGS} - \epsilon_{i\theta}^{SGS} + \Pi_{i\theta}^{SGS}}{\sqrt{(K^{SGS}K_\theta^{SGS})}} \tag{6}$$

where P_K^{SGS} and ϵ_K^{SGS} are the production and dissipation of the SGS kinetic energy, respectively, and where P_θ^{SGS} and ϵ_θ^{SGS} denote the production and dissipation of the SGS scalar intensity. D_i^ξ is the diffusion of the normalised SGS flux, ξ_i. If we assume that the weak equilibrium assumption is valid, i.e. if the left hand side of 6 is negligible ($D\xi_i/Dt - D_i^\xi = 0$), we can model the unknown terms $\Pi_{i\theta}^{SGS} - \epsilon_{i\theta}^{SGS}$ in the same way as in the Reynolds averaged case but in terms of q_i, τ_{ij} and filtered gradients instead of $\langle u_i'\theta'\rangle$, $\langle u_i'u_j'\rangle$ and mean gradients

$$\begin{aligned}\Pi_{i\theta}^{SGS} - \epsilon_{i\theta}^{SGS} =& -\left(c_{1\theta} + c_{5\theta}\frac{K^{SGS}}{\epsilon_K^{SGS}K_\theta^{SGS}}q_k\frac{\partial\tilde{\theta}}{\partial x_k}\right)q_i\frac{\epsilon_K^{SGS}}{K^{SGS}}\\ &+ c_{2\theta}q_j\frac{\partial\tilde{u}_i}{\partial x_j} + c_{3\theta}q_j\frac{\partial\tilde{u}_j}{\partial x_i} + c_{4\theta}\tau_{ij}\frac{\partial\tilde{\theta}}{\partial x_j}\end{aligned}$$

With $c_{5\theta} = 1/2$ (see Wikström et al. (2000)) we obtain a linear system of equations

$$\begin{aligned}A_{ij}q_j &= -\tau^{SGS}c_1\tau_{ij}\frac{\partial\tilde{\theta}}{\partial x_j}\\ A_{ij} &= G\delta_{ij} + c_S S_{ij} + c_\Omega\Omega_{ij}\end{aligned} \tag{7}$$

where $\tau^{SGS} = K^{SGS}/\epsilon_K^{SGS}$ is the time scale of the subgrid velocity field, $c_1 = (1 - c_{4\theta})$ is a model constant, and

$$G = \frac{1}{2}\left(2c_{1\theta} - 1 - \frac{1}{r} + \frac{P_K^{SGS}}{\epsilon_K^{SGS}}\right) \tag{8}$$

The normalised filtered rates of strain and rotation tensors are defined as $S_{ij} = \tau^{SGS}\left(\tilde{u}_{i,j} + \tilde{u}_{j,i}\right)/2$ and $\Omega_{ij} = \tau^{SGS}\left(\tilde{u}_{i,j} - \tilde{u}_{j,i}\right)/2$. As a first approximation for this type of model we use a constant time scale ratio, r, and an ensemble averaged time scale, τ^{SGS}

$$\begin{aligned} r &= \frac{K^{SGS}/\epsilon_K^{SGS}}{K_\theta^{SGS}/\epsilon_\theta^{SGS}} \approx 0.7 \\ \tau^{SGS} &\approx \frac{\langle K^{SGS}\rangle}{\langle \epsilon_K^{SGS}\rangle} \end{aligned} \tag{9}$$

Thereby, we do not need to solve the transport equation of the subgrid scalar intensity, K_θ^{SGS}, and the time scale based on $\langle K^{SGS}\rangle$ can be estimated from dimensional arguments, see section 4. In homogeneous flows the ensemble average denoted by $\langle\rangle$ is the same as a volume avarage but inhomogeneous flows require local ensemble averaging.

If A_{ij} is invertible we obtain an explicit algebraic expression for the subgrid scalar flux

$$q_i = -\tau^{SGS} c_1 A_{ij}^{-1} \tau_{jk} \frac{\partial \tilde{\theta}}{\partial x_k} \tag{10}$$

where (boldface denotes matrix notation)

$$\mathbf{A^{-1}} = \frac{(G^2 - \frac{1}{2}Q_1)\mathbf{I} - G(c_S\mathbf{S} + c_\Omega\mathbf{\Omega}) + (c_S\mathbf{S} + c_\Omega\mathbf{\Omega})^2}{G^3 - \frac{1}{2}GQ_1 + \frac{1}{2}Q_2} \tag{11}$$

Here, $Q_1 = c_S^2 tr(\mathbf{S}^2) + c_\Omega^2 tr(\mathbf{\Omega}^2)$, $Q_2 = (2/3)c_S^3 tr(\mathbf{S}^3) + 2c_S c_\Omega^2 tr(\mathbf{S\Omega}^2)$ where $c_S = (1 - c_{2\theta} - c_{3\theta})$ and $c_\Omega = (1 - c_{2\theta} + c_{3\theta})$ are constant model parameters.

It is beyond the scope of this study to prove that the weak equillibrium assumption is valid for ξ_i and that it is appropriate to model the unknown terms, $\Pi_{i\theta}^{SGS} - \epsilon_{i\theta}^{SGS}$, in the same manner as in the EASFM, but with filtered quantities instead of Reynolds averaged quantities. Nevertheless, we claim that we end up with a reasonable final expression (10) for the SGS scalar flux. The modelled SGS flux is in general not aligned with the resolved scalar gradient. In fact it can be rewritten as a mixed model including an eddy diffusion term

$$q_i = -\tau^{sgs} c_1 \left(\left(A_{ij}^{-1}\tau_{jk} - \delta_{ik}\frac{A_{lj}^{-1}\tau_{jl}}{3}\right)\frac{\partial \widetilde{\theta}}{\partial x_k} + \frac{A_{kj}^{-1}\tau_{jk}}{3}\frac{\partial \widetilde{\theta}}{\partial x_i}\right) \tag{12}$$

Moreover, there is a strong influence of the SGS stresses and the amplification tensor A_{ij}^{-1} involves information about both the resolved rate of strain and the

resolved rotation rate tensor.

In a rotating frame of reference embedded with the flow the Coriolis term will modify the advection as well as the production of the SGS scalar flux according to

$$\begin{aligned} \frac{D\xi_i}{Dt} &= \frac{\partial \xi_i}{\partial t} + \tilde{u}_j \frac{\partial \xi_i}{\partial x_j} + \epsilon_{ikj}\Omega_k \xi_j \\ P_{i\theta} &= -q_j \frac{\partial \tilde{u}_i}{\partial x_j} - \tau_{ij} \frac{\partial \tilde{\theta}}{\partial x_j} - \epsilon_{ikj}\Omega_k q_j \end{aligned} \tag{13}$$

Hence, the weak equillibrium assumption corresponds to $\partial \xi_i/\partial t + \tilde{u}_j \partial \xi_i/\partial x_j - D_i^{\xi} + \epsilon_{ikj}\Omega_k \xi_j = 0$ in a rotating frame. The modified production term can be accounted for by modifying Ω_{ij} into the frame invariant

$$\Omega_{ij}^{*} = \Omega_{ij} + \tau^{SGS}\epsilon_{ikj}\Omega_k \tag{14}$$

This is the only modification needed to extend the model to rotating flows. In RANS of fully developed rotating turbulent flows it is a better approximation to keep the Coriolis contribution resulting from the transformation to the rotating frame as an approximation of the advection, see Gatski and Wallin (2004). The motivation for this is that the flow is statistically homogeneous in the rotating frame only. However, there is no obvious reason to believe that the same applies for LES where SGS field is advected by the instantanous filtered velocity field, and where the filtered statistics cannot be considered to be homogeneous in any frame of reference. The frame invariant formulation in (13) and (14) is thus the most appropriate choice.

4. Simulations

The performance of the new model was tested in rotating homogeneous shear flow, with the model parameters chosen as $c_s = 0.50$, $c_r = 0.6$, $c_1 = 2.2$, and $c_{1\theta} = 3.6$. These parameters were found to give the best description of the the magnitude and anisotropy of the scalar variance SGS dissipation. No backscatter was allowed. Model predictions causing negative SGS disspation were put to zero. The linear system of equations (7) can become close to singular at some grid points. In the present LES it was nescessary to neglect about 1% of the model predictions that had the largest condition number.

The filtered incompressible Navier-Stokes equations with a constant uniform shear, $U_i = Sx_3\delta_{i1}$, and the passive scalar equation with a scalar gradient, $S_i^{\theta} = \delta_{i3}$, were solved using a pseudo spectral code with a third order Runge-Kutta method for time advancement. LES with 64^3 and 96^3 grid-points were performed in a periodic box with the dimensions $4\pi \times 3\pi \times 2\pi$ starting from a random isotropic velocity field with a prescribed shape of the energy spectrum.

The initial scalar field in the simulations was without fluctuations. Three different models for the SGS flux were used: The new explicit model, the eddy diffusion model with a constant Prandtl number, $Pr_T = 0.38$, number and the mixed similarity model

$$q_i = -\frac{\nu_T}{Pr}\frac{\partial\tilde{\theta}}{\partial x_i} + c_{sim}\left(\widehat{\tilde{u}_i\tilde{\theta}} - \hat{\tilde{u}}_i\hat{\tilde{\theta}}\right) \tag{15}$$

with $Pr_T = 0.65$. These model parameters were found to give the best description of the the magnitude of the scalar variance SGS dissipation at $R = -1$. The scale similarity constant was set to $c_{sim} = 1.0$ as in the dynamic mixed model by Zang et al. (1993). The hat operator denotes a Gaussian filter with $\hat{\Delta} = 2\Delta$. The Smagorinsky model was used as the subgrid model for the velocity field. As it relies on the equilibrium assumption $\langle P_K^{SGS}\rangle \approx \langle\epsilon_K\rangle$ we used $P_K^{SGS}/\epsilon_K^{SGS} = 1$, in the SGS scalar flux model. The length scale, Δ, of the subgrid field is known, and it was used to estimate τ^{SGS}. From dimensional arguments we have

$$\tau^{SGS} = C\left(\Delta^2/\langle\Pi\rangle\right)^{1/3} \tag{16}$$

where C is a constant of order 1 and $\Pi = -\tau_{ij}\tilde{S}_{ij}$ is the SGS energy dissipation. The initial non-dimensional shear rate was chosen as $S\tilde{K}/\tilde{\epsilon} = 1.2$, and the initial turbulence Reynolds number was $Re_T = \tilde{K}^2/(\tilde{\epsilon}\nu) = 33000$.

The LES results on the equillibrium values of the direction of the scalar flux (section 5.1) and the relative intensity of the scalar fluctuations (section 5.3) were compared with the non-filtered DNS data by Brethouwer and Matsuo (2005). In the DNS the initial Reynolds number, $Re_T = 135$, is lower than in the LES. However, we believe that the equillibrium values considered are independent of the Reynolds number.

5. Results

5.1. *Direction of the resolved and SGS scalar flux*

The direction of the turbulent scalar flux is defined as

$$\alpha_f = atan\left(\frac{\langle\tilde{\theta}'\tilde{u}_3'\rangle}{\langle\tilde{\theta}'\tilde{u}_1'\rangle}\right) \tag{17}$$

where $\tilde{u}_i'$ and $\tilde{\theta}'$ denote the fluctuating velocity and scalar components, and where $\langle\tilde{\theta}'\tilde{u}_1'\rangle$ and $\langle\tilde{\theta}'\tilde{u}_3'\rangle$ are the mean turbulent scalar fluxes in the x_1 and x_3 direction, respectively. The scalar flux is a first order statistic in the scalar and we can only expect small differences in between the models. In figure 1 the development of α_f is seen to depend strongly on the rotation number. The angle α_f in the LES with the eddy diffusivity model, the mixed model and the new explicit model approaches the same equilibrium values and the results yield good agreement with DNS results of Brethouwer and Matsuo and Rogers

et al. (1989). The ratio of the mean turbulent diffusivity to the molecular diffusivity is about 500 showing that the similarities between the predictions of the SGS models are not the result of a low Reynolds number.

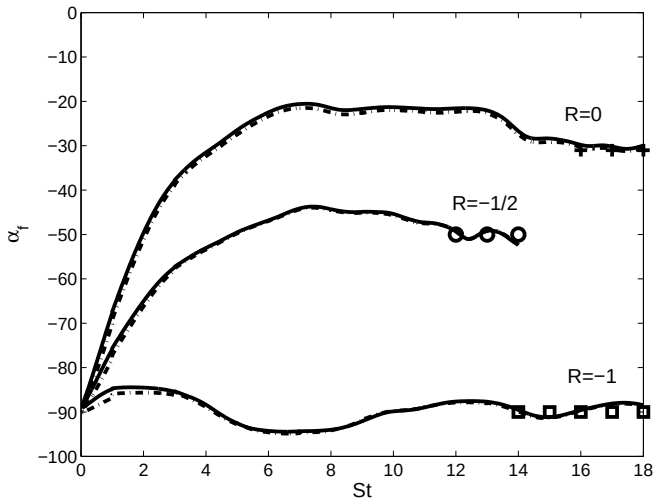

FIGURE 1. *The direction of the mean turbulent scalar flux. New model, solid line; eddy diffusion model, dashed line; mixed model, dotted line; DNS data, symbols.*

The very small differences between the model predictions can be understood by considering the transport equation for the scalar flux in homogeneous flows

$$\begin{aligned}
\frac{D}{Dt}\langle\tilde{\theta}^{'}\tilde{u}_i^{'}\rangle &= P_{i\theta} + \Pi_{i\theta} - \epsilon_{i\theta} - \epsilon^q_{i\theta} - \epsilon^\tau_{i\theta} \\
P_{i\theta} &= -\langle u_i^{'}u_j^{'}\rangle\frac{\partial\Theta}{\partial x_j} - \langle\theta^{'}u_j^{'}\rangle\frac{\partial U_i}{\partial x_j} \\
\epsilon^q_{i\theta} &= -\langle q_j\frac{\partial u_i^{'}}{\partial x_j}\rangle \\
\epsilon^\tau_{i\theta} &= -\langle\tau_{ij}\frac{\partial\theta^{'}}{\partial x_j}\rangle
\end{aligned} \tag{18}$$

where $P_{i\theta}$ is the production, $\Pi_{i\theta}$ is the pressure scalar gradient correlation, and $\epsilon_{i\theta}$ is the molecular dissipation. The terms $\epsilon^q_{i\theta}$ and $\epsilon^\tau_{i\theta}$ are the SGS dissipation of the scalar flux. The only way that the scalar SGS model explicitly enters the equation is through the SGS dissipation term, $\epsilon^q_{i\theta}$. By defining the ratio

$$H_\beta = \frac{\epsilon^q_{\beta\theta}}{P_{\beta\theta}} \tag{19}$$

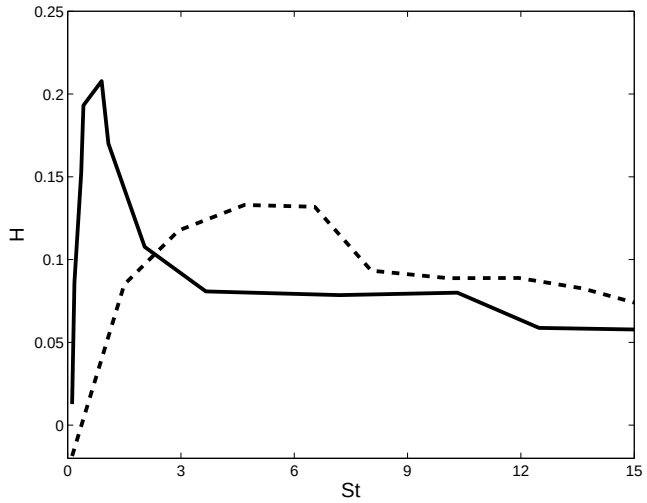

FIGURE 2. *The ratio H_i at $R = 0$ according to the eddy diffusion model. H_1 dashed line; H_3, solid line*

we can quantify the influence of the SGS flux model on the mean scalar flux. From figure 2 we can see that H is very small for large shear times. This explains why the choice of SGS model has only a very small influence on the equilibrium values of α_θ. The mean scalar flux simply grows much larger than the SGS scalar flux.

Next we turn our attention to the SGS scalar flux. The mean SGS flux does not affect the scalar field in homogeneous flow, but it is a well defined property which is of some importance in inhomogeneous flows. An appropriate SGS model should be able to predict properties of $\langle q_i \rangle$. Similar to the direction of the resolved scalar flux, we define the direction of the subgrid scalar flux as

$$\alpha_\theta = atan\left(\frac{\langle q_3 \rangle}{\langle q_1 \rangle}\right) \tag{20}$$

From figure 3 we can see that the eddy diffusivity model predicts a subgrid flux which is almost aligned with the transverse mean scalar gradient, whereas the direction of $\langle \hat{q}_i \rangle$ according to the new model depends strongly on the rotation number with a significant subgrid flux component in the streamwise direction at $R = 0$ and at $R = -1/2$. It resembles the way the direction of the mean scalar flux depends on the rotation number. The results of the scale similarity part of the mixed model in figure 3 respond to rotation in a similar way as those of the new explicit model with approximate agreement of the equillibrium values at $R = 0$ and $R = -1/2$. However, the ad hoc combination of a

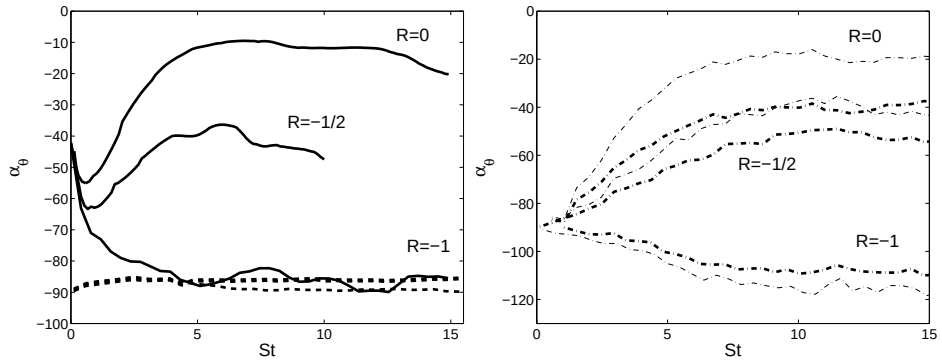

FIGURE 3. *The direction in degrees of the mean SGS scalar flux at* $R = 0,\ -1/2$ *and* $R = -1$. *New model, solid line; eddy diffusion model, dashed line; mixed model, dashed-dotted line; scale similarity part of the mixed model, thin dashed-dotted line.*

scale similarity part and an eddy diffusion part changes the direction of $\langle \hat{q}_i \rangle$ with about $15 - 20$ degrees towards the transverse mean scalar gradient.

Hence, the predictions of the new explicit model and the mixed model respond to rotation in a similar way as the large scale turbulence flux. This is relistic since it is well known that the anisotropy of a passive scalar field persists down to very small scales.

5.2. *Anisotropy of the scalar variance SGS dissipation*

In contrast to the anisotropy of the energy SGS dissipation the anisotropy of the scalar variance SGS dissipation is known to persist down to very small filter scales, see Kang and Meneveau (2001). Similar to Kang and Meneveau we define the isotropy measure

$$I_\theta = \frac{\langle q_1 \frac{\partial \tilde{\theta}'}{\partial x_1} \rangle}{\langle q_3 \frac{\partial \tilde{\theta}'}{\partial x_3} \rangle} \tag{21}$$

which is equal to one in case of isotropy.

The time dependence of I_θ according to the new explicit model, the eddy diffusivity model, and the mixed similarity model is presented in figure 4 for the non rotating case $R = 0$. In agreement with the results of Kang and Meneveau (2001) the anisotropy predicted by the eddy diffusivity model is aligned with that of the mean squared scalar gradient. The result is rather anisotropic with a large $\langle q_3 \frac{\partial \tilde{\theta}'}{\partial x_3} \rangle$-component. I_θ predicted by the mixed similarity model is also

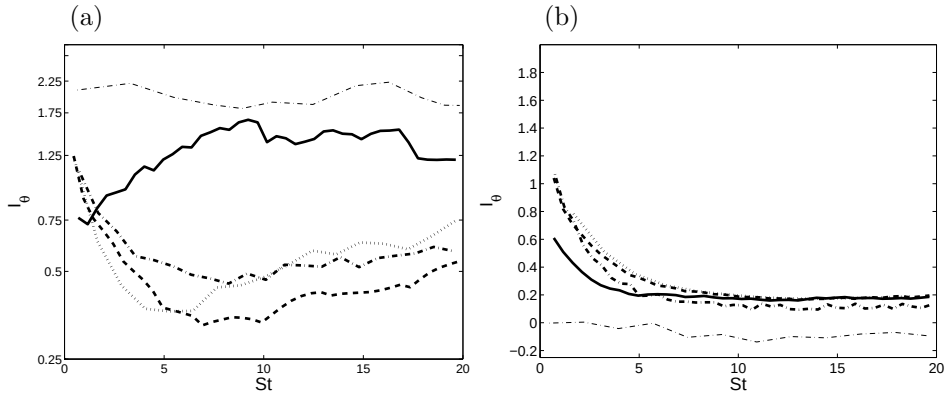

FIGURE 4. *The anisotropy of the SGS dissipation at (a): $R = 0$ and at (b): $R = -1$. New model, solid line; eddy diffusion model, dashed line; mixed model, dash-dotted line; scale similarity part, thin dash-dotted line with; squared scalar gradient, dotted line.*

approximately aligned with the mean squared gradient. This is due to the eddy dffusion part which dominates the SGS dissipation. On the contrary the new explicit model and the scale similarity part of the mixed model yeild $I_\theta > 1$, i.e. there is a sigificant $\langle q_1 \frac{\partial \tilde{\theta}'}{\partial x_1} \rangle$-component of the SGS-dissipation. With the suggested set of model parameters the new explicit model predicts $I_\theta \approx 1.3$. The scale similarity part of the mixed model is more anisotropic with $I_\theta \approx 2.0$. At the rotation number $R = -1$ (figure 4) all models predict $I_\theta \approx 0.2$. Apparently, anisotropy of the SGS dissipation resulting from the new explicit model has the ability to respond to system rotation in a much more pronounced way than eddy diffusion model and the mixed model.

The anisotropy of the SGS dissipation according to the new model is strongly affected by the model parameter c_Ω. Figure 5 shows I_θ as a function of c_Ω/c_S at $R = 0$, $St = 10$ and with $c_S = 0.5$. At small or negative c_Ω/c_S the anisotropy of the new model resembles that of the eddy diffusion model with a large $\langle q_3 \frac{\partial \tilde{\theta}'}{\partial x_3} \rangle$-component. As c_Ω/c_S increases I_θ becomes more similar to that of the scale similarity part of the mixed model. I_θ is also more sensitive to c_Ω when $c_\Omega \approx c_S$. We do not recommend the use of $c_S > 0.52$. In that case the explicit model expression can easily become singular, see Wikström et al. (2000).

5.3. *Intensity measure*

One of the basic demands on an SGS model is that it produces the right amount of mean dissipation. We compare the amount of mean dissipation produced by

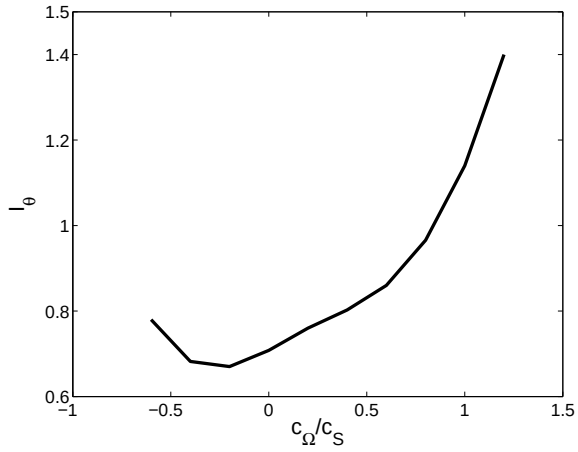

FIGURE 5. *The anisotropy of the SGS dissipation as a function of* c_Ω/c_S *at* $St = 10$ *and* $R = 0$ *according to the new explicit model.*

the SGS models under the influence of rotation by studying the length scale ratio formed by the scalar length scale $\tilde{K}_\theta^{1/2}/S^\theta$ and the velocity length scale $\tilde{K}^{1/2}/S$

$$B = \frac{\tilde{K}_\theta^{1/2}/S^\theta}{\tilde{K}^{1/2}/S} \tag{22}$$

where $\tilde{K}_\theta$ is half the scalar variance, $\tilde{K}$ is the turbulence kinetic energy, and S^θ is the magnitude of mean the scalar gradient. B represents the relative intensity of the scalar fluctuations compared to the velocity fluctuations. According to Rogers et al. (1989) the equillibrium values of B depend on the Prandtl number and the orientation of the mean scalar gradient but is relativly insensitive to other parameters such as the Reynolds number.

It can be seen from figure 6 that B approaches different equilibrium values depending on the rotation number. The resolution is 64^3. We calibrated all models to fit with the unfiltered DNS data by Brethouwer and Matsuo (2005) at the rotation number $R = -1$ where all three models predicts qualitatively the same anisotropy of the SGS dissipation. The resulting model parameters were presented in section 4. $\tilde{K}_\theta$ and $\tilde{K}$ are large scale statistics and we assume that the effect of a filter is small on the ratio B. (In fact the effect of a filter cancels if the fraction of resolved scalar intensity to the full scalar intensity is equal to the fraction of resolved turbulent intensity to the full turbulent intensity.) All model parameters were kept constant and independent of the rotation number.

From the results in figure 6 we see that the eddy diffusivity model and the mixed model become too dissipative at $R = 0$ whereas the new explicit model

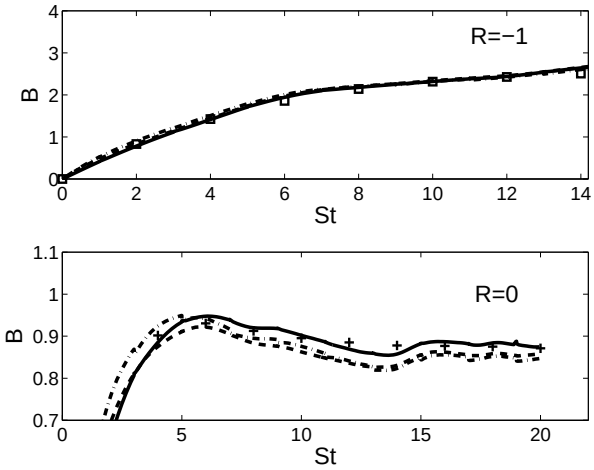

FIGURE 6. *Intensity ratio measure B at $R = 0$ and $R = -1$. Eddy diffusion model, dashed line; new model, solid line; mixed model, dotted line; DNS, symbols.*

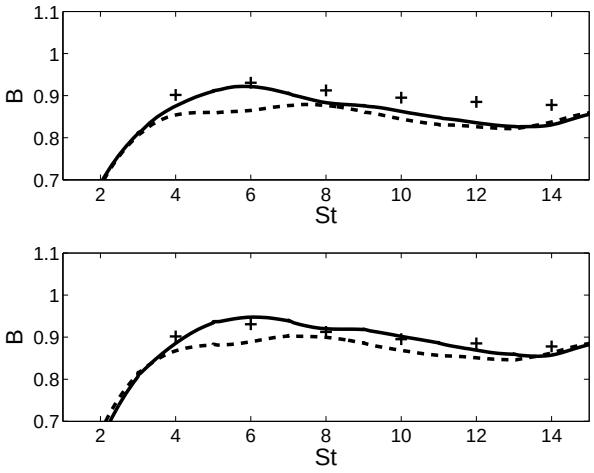

FIGURE 7. *Filter scale dependence of the intensity measure B at $R = 0$ according to the eddy diffusion model (upper figure) and the new model (lower figure). $\Delta/\eta = 1400$, solid line; $\Delta/\eta = 990$, dashed line; DNS, symbols.*

compares well with the DNS data at both rotation numbers. Hence the new model provides for a better description of the mean dissipation than both the eddy diffusion model and the mixed model for the suggested model parameters.

The model parameter c_S has a stronger impact on the amount of SGS dissipation than c_Ω. Increasing c_S increases the SGS dissipation whereas increasing c_Ω slightly decreases the dissipation. To find out whether it is appropriate or not to use constant model parameters (that do not depend on the filter scale) we compare the ratio B calculated at two different filter scales. Figure 7 shows that the differences in the prediction of B owing to the filter scale are not larger for new explicit model than for the eddy diffusion model, at $R = 0$. This indicates that constant model parameters are about as appropriate as a turbulent Prandtl number that does not depend on the filter scale.

6. Conclusions

A new explicit SGS scalar flux model based on a modelled transport equation for the subgrid scalar flux is proposed and its performance tested in homogeneous shear flow subject to rotation. The new model is based on the same kind of methodology that leads to the EASFM for the Reynolds avaraged flux.

The direction of the mean SGS scalar flux predicted by the new explicit model is similar to that of the mixed similarity model. Both models respond to rotation in a more realistic way than the eddy diffusion model. Moreover the new explicit model provides for a better description of the anisotropy of the SGS dissipation than both the eddy diffusion model and the mixed similarity model that predicts an anisotropy similar to that of the squared scalar gradient. The contribution to I_θ by the scale similarity part improves the results of the mixed model. Despite that, the mixed model fails to predict I_θ due to the very strong dissipative nature of the eddy diffusion part. The new model also provides for a better description of the mean SGS dissipation than both the eddy diffusion model and the mixed model at the two rotation numbers considered.

References

Brethouwer G, Matsuo Y. 2005. DNS of rotating homogeneous shear flow and scalar mixing. Proc. 4th Int. Symp. on Turbulence and Shear Flow Phenomena (TSFP4), Williamsburg, USA. Editors: J A C Humphrey et al.

Kang, H S, Meneveau, C. 2001. Passive scalar anisotropy in a heated turbulent wake, new observations and implications for large eddy simulations. *J. Fluid Mech.* **442**, 161-170.

Gatski T, Wallin S. 2004. Extending the weak-equilibrium condition for algebraic Reyolds stress models to rotatingand curved flows. *J. Fluid Mech.* **518**, 147-155.

Cerutti S. , Meneveau, C. 1998. Intermittency and relative scaling of subgrid scale energy dissipation in isotropic turbulence. *Phys. of Fluids* **10** , 928-937.

Wikström, P.M.; Wallin, S.; Johansson, A.V. 2000. Derivation and investigation of a new algebraic model for the passive scalar flux. *Phys. Fluids* **12**, 688-702.

Zang Y, Street R, Koseff J. 1993. A dynamic subgrid-scale model and its application to turbulent recirculating flows. *Phys. Fluids A* **5**, 3186-3196.

Calmet I, Magnaudet J. 1997. Large-eddy simulations of high-Schmidt number mass transfer in a turbulent channel flow. *Phys. Fluids* **9**, 438-455.

Marstorp L, Brethouwer G, Johansson A. 2005. Stochastic SGS modelling in rotating homogeneous shear flow with a passive scalar. To appear in *Proc. Direct and Large Eddy simulations 6* (**DLES6**) , Poitiers, France.

Bardina J Ferzinger J.H Reynolds, W.C. 1983. Improved turbulence models based on large eddy simulation of homogeneous incompressible flows. Technical report No. **TF-19** Stanford University.

Rogers M M, Mansour N N, Reynolds W C. 1989. An algebraic model for the turbulent flux of a passive scalar. *J. Fluid Mech.* **203**, 77-101.

3

Paper 3

A code for large-eddy simulation of rotating homogeneous shear flow with passive scalars

By Linus Marstorp, Geert Brethouwer & Arne V. Johansson

1. Introduction

Although homogeneous shear flow is an idealised flow without any spatial gradients of the turbulent correlations, it approximates different regions of inhomogeneous and wall bounded shear flows depending on the ratio between the inverse shear rate and the turbulence macro scale. For example, some of the turbulence structures in homogeneous shear flow at high shear rates are similar to those found in the near wall region of boundary layers and turbulent channel flow, see Rogers and Moin (1987). The present code for numerical simulation of homogeneous shear flow is based on the Rogallo (1981) method, which has been utilised in several studies. Bardina et al. (1983) evaluated their scale similarity model in large eddy simulations of homogeneous shear flow using the Rogallo method. A more recent example is the DNS by Brethouwer and Matsuo (2005) who studied the effect of rotation on passive scalar mixing.

A passive scalar is mixed by flow field without affecting the flow in any way. In experiments the passive scalar is often represented by small temperature fluctuations, see for example the experiments by Tavoularis and Corrsin (1981) or Kang and Meneveau (2001). Rogers et al. (1989) were among the first to include a passive scalar into numerical simulation of homogeneous shear flow. A homogeneous scalar field requires a constant mean scalar gradient. Rogers et al. imposed a mean scalar gradient in different directions and derived a scalar flux model based on the results of their DNS.

The present report describes the large-eddy simulation code used in the present work.

2. Governing equations

We wish to solve the Navier-Stokes equations for the fluctuating velocity field, u_i, with an imposed mean velocity profile $U_i = Sx_3\delta_{i1}$, and the equation for a passive scalar fluctuation, θ with a constant mean scalar gradient $\partial\Theta/\partial x_i = G_i$

in a rotating frame. The governing equations read

$$\begin{aligned}
&\frac{\partial u_i}{\partial t} + Sx_3\frac{\partial u_i}{\partial x_1} + \frac{\partial u_i u_j}{\partial x_j} + u_3 S\delta_{i1} = -\frac{1}{\rho}\frac{\partial p}{\partial x_i} + \nu\frac{\partial^2 u_i}{\partial x_j x_j} - 2\epsilon_{ijk}\Omega_j u_k \\
&\frac{\partial u_i}{\partial x_i} = 0 \\
&\frac{\partial \theta}{\partial t} + Sx_3\frac{\partial \theta}{\partial x_1} + \frac{\partial \theta u_j}{\partial x_j} + u_j G_j = \frac{\nu}{Pr}\frac{\partial^2 \theta}{\partial x_j x_j}
\end{aligned} \tag{1}$$

where p includes both the pressure and the centrifugal force. Ω_i is the system rotation vector, ν is the viscosity, Pr is the Prandtl number, and ϵ_{ijk} is the alternating tensor.

It is convenient to have periodic boundary conditions in all directions for the fluctuating quantities. In the x_1-direction they are

$$\begin{aligned}
u_i(x_1 + L_1, x_2, x_3) &= u_i(x_1, x_2, x_3) \\
\theta(x_1 + L_1, x_2, x_3) &= \theta(x_1, x_2, x_3)
\end{aligned} \tag{2}$$

where L_1 is the streamwise box size. Periodic boundary conditions satisfy the restriction of homogeneity and are easy to implement. However, it is not possible to apply periodic boundary conditions to (1) due to the non constant factor Sx_3. The governing equations have to be transformed to a frame that moves with the mean flow in order to enable the periodic boundary conditions.

2.1. *Coordinate transformation*

The coordinate transformation to a moving frame can be written as a matrix-vector multiplication

$$x_i^{'} = B_{ij}x_j \tag{3}$$

where $B_{ij} = \delta_{ij} - St\delta_{i1}\delta_{j3}$. The governing equations have to be rewritten in terms of the new coordinates. All spatial derivatives have to be transformed

$$\partial x_i^{'} = B_{ij}\partial x_j \tag{4}$$

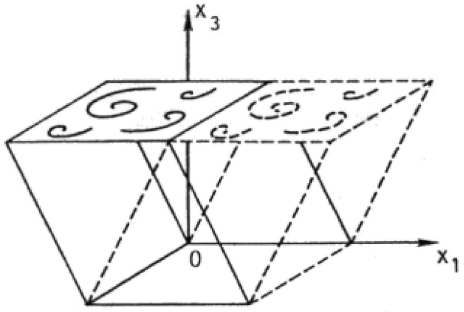

FIGURE 1. *The moving frame.*

By applying (4) and the time transformation $t^{'} = t$ to (1) we obtain the governing equations in the moving frame

$$\frac{\partial u_i}{\partial t'} + (\delta_{kj} - St^{'}\delta_{k1}\delta_{j3})\frac{\partial u_i u_j}{\partial x_k^{'}} = -\frac{\partial p}{\partial x_j^{'}}\left(\delta_{ij} - St^{'}\delta_{i3}\delta_{j1}\right) - Su_3\delta_{i1} +$$
$$+ \nu\frac{\partial^2 u_i}{\partial x_j^{'}x_k^{'}}\left(\delta_{jk} - 2St^{'}\delta_{j1}\delta_{k3} + (St^{'})^2\delta_{j1}\delta_{k1}\right) - 2\epsilon_{ijk}\Omega_j u_k$$
$$\frac{\partial u_i}{\partial x_j^{'}}\left(\delta_{ij} - St^{'}\delta_{i3}\delta_{j1}\right) = 0$$
$$\frac{\partial \theta}{\partial t'} + (\delta_{kj} - St^{'}\delta_{k1}\delta_{j3})\frac{\partial u_j\theta}{\partial x^{'}{}_k} = -u_i G_i + \frac{\nu}{Pr}\frac{\partial^2\theta}{\partial x_j^{'}\partial x_k^{'}}\left(\delta_{jk} - 2St^{'}\delta_{j1}\delta_{k3} + (St^{'})^2\delta_{j1}\delta_{k1}\right) \tag{5}$$

Note that if the velocity vector is transformed according $u_i^{'} = B_{ij}u_j$, the nonlinear term that depends on St disappears. Bardina et al. (1983) implemented the equations in that way. The moving frame is sketched in figure 1.

The domain has to be re-meshed before it becomes too distorted to contain the largest turbulence structures. The time interval for re-meshing depends on box size ratio L_1/L_3 and is performed at the nondimesional shear times

$$St = \frac{L_1}{L_3}\left(\frac{1}{2}, \frac{3}{2}, \frac{5}{2}\cdots\right) \tag{6}$$

In physical space the re-mesh corresponds to the shift

$$x^{'}_{i(new)} = x^{'}_{i(old)} - \frac{L_1}{L_3}x^{'}_3\delta_{i1}$$
$$u_i^{(new)}\left(x^{'}_{i(new)}\right) = u_i^{(old)}\left(x^{'}_{i(new)} + \frac{L_1}{L_3}x^{'}_3\delta_{i1}\right) \tag{7}$$

2.2. *Filtered equations*

A Large Eddy Simulation is an under-resolved numerical simulation of the Navier-Stokes equations in which the influence of the non-resolved scales has to be modelled. To remove the small scales a filtering operation is applied to the governing equations using a convolution filter

$$\tilde{u}(\mathbf{x},t) = \int_{\mathbb{R}^3} G(\mathbf{x}-\mathbf{y})u(\mathbf{y},t)d\mathbf{y} \tag{8}$$

which commutes with the differential operator. The filtered equations are

$$\begin{aligned}
&\frac{\partial \tilde{u}_i}{\partial t'} + (\delta_{kj} - St'\delta_{k1}\delta_{j3})\frac{\partial \tilde{u}_i\tilde{u}_j}{\partial x_k'} = -\frac{\partial p}{\partial x_j'}\left(\delta_{ij} - St'\delta_{i3}\delta_{j1}\right) - S\tilde{u}_3\delta_{i1} + \\
&+ \nu\frac{\partial^2 \tilde{u}_i}{\partial x_j' x_k'}\left(\delta_{jk} - 2St'\delta_{j1}\delta_{k3} + (St')^2\delta_{j1}\delta_{k1}\right) - 2\epsilon_{ijk}\Omega_j\tilde{u}_k - (\delta_{kj} - St'\delta_{k1}\delta_{j3})\frac{\partial \tau_{ij}}{\partial x_k'} \\
&\frac{\partial \tilde{u}_i}{\partial x_j'}\left(\delta_{ij} - St'\delta_{i3}\delta_{j1}\right) = 0 \\
&\frac{\partial \tilde{\theta}}{\partial t'} + (\delta_{kj} - St'\delta_{k1}\delta_{j3})\frac{\partial \tilde{u}_j\tilde{\theta}}{\partial x'_k} = -\tilde{u}_i G_i + \frac{\nu}{Pr}\frac{\partial^2 \tilde{\theta}}{\partial x_j' \partial x_k'}\left(\delta_{jk} - 2St'\delta_{j1}\delta_{k3} + (St')^2\delta_{j1}\delta_{k1}\right) \\
&- (\delta_{kj} - St'\delta_{k1}\delta_{j3})\frac{\partial q_j}{\partial x_k'}
\end{aligned} \tag{9}$$

where the SGS stress, $\tau_{ij} = \widetilde{u_i u_j} - \tilde{u}_i\tilde{u}_j$, and the SGS scalar flux, $q_i = \widetilde{u_i\theta} - \tilde{u}_i\tilde{\theta}$, have to be modelled in order to close the system of equations.

3. Numerical method

To solve the governing equations, a pseudo-spectral method is applied, which means that the nonlinear terms are computed in physical space whereas the spatial derivatives are computed in Fourier space. Hence, the solution has to be transformed back and forth between the two spaces using a 3D discrete Fourier transform

$$\begin{aligned}
\hat{f}(\mathbf{k}) &= \frac{1}{N_1N_2N_3}\sum_{n_3=0}^{N_3-1}\sum_{n_2=0}^{N_2-1}\sum_{n_1=0}^{N_1-1} f(\mathbf{x})e^{-ix_3(n_3)k_3}e^{-ix_2(n_2)k_2}e^{-ix_1(n_1)k_1} \\
x_\alpha(n_\alpha) &= \frac{2\pi n_\alpha}{N_\alpha}, \qquad -N_\alpha/2 \geq k_\alpha \leq N_\alpha/2 - 1
\end{aligned} \tag{10}$$

The discrete Fourier transform is computed using the Fast Fourier Transform, FFT, algorithm. One of the main advantages of the spectral method is that

the transform of the spatial derivatives can be accurately computed in Fourier space as

$$\widehat{\frac{\partial u_i}{\partial x_j}}(k_1,k_2,k_3) = ik_j\hat{u}_i(k_1,k_2,k_3) \tag{11}$$

3.1. *Dealiasing*

Aliasing errors appears when the nonlinear terms are computed in physical space. In the one-dimensional case the product of two variables with length N in Fourier space contains wave numbers in a twice as large range $2N$. Some of the high wavenumber nodes produces spurious aliased waves when the product is transformed back to Fourier space using a transform of length N.

The aliasing error can be removed by either truncation or by phase shift. If the one-dimensional discrete Fourier transform of length N is truncated to length $2N/3$ the alias error will disappear from the product. This is usually referred to as the 2/3 rule, see for example Rogallo (1981). Truncation according to the 2/3 rule is computationally expensive, because much of the high wave number information is lost. In the phase shift method each Fourier mode is multiplied with a phase shift factor. It damps the aliasing error without affecting the alias-free part of the solution, see Rogallo (1981). In the present code a combination of truncation and phase shifts is applied. All Fourier modes larger than $|\mathbf{k}|^2/|\mathbf{k}|^2_{max} = 8/9$ are truncated to zero and the nonlinear terms are phase shifted at each time step.

3.2. *Time advancement*

In Fourier space the governing equations for the velocity components and the passive scalar can be put in the form

$$\frac{\partial \hat{f}}{\partial t} = F(t,\hat{f},\mathbf{k}) \tag{12}$$

The time advancement is then performed in Fourier space using the a third order low-storage Runge Kutta method proposed by Williamson (1980)

$$\begin{aligned} &f_0 = \hat{f}^{(n)} \\ &G_j = a_j G_{j-1} + \Delta t F(t_n, f_{j-1}, \mathbf{k}) \qquad j = 1\ldots 3 \\ &f_j = f_{j-1} + b_j G_j \\ &\hat{f}^{(n+1)} = f_3 \end{aligned} \tag{13}$$

where $a_1 = 0$, $a_2 = (3\sqrt{6} - 13)/10$, $a_3 = -2(3 + \sqrt{6})/9$, $b_1 = (6 - \sqrt{6})$, $b_2 = (6 + \sqrt{6})$, and $b_3 = 1/2$. Only two levels of storage are needed. The time step is determined by prescribing the CFL-number, $CFL = \sqrt{3}$.

3.3. *Initial conditions*

The initial condition for the velocity field is random and isotropic with a prescribed shape of the energy spectrum. It is calculated in Fourier space in three steps: First, all modes are given random amplitude and random phase from a uniform distribution. Thereby the initial field (u^*, v^*, w^*) is isotropic. The velocity field is then made divergence free by the transformation

$$\begin{aligned} \hat{u} &= \hat{u}^* - k_1 \frac{(k_1\hat{u}^* + k_2\hat{v}^* + k_3\hat{w}^*)}{|\mathbf{k}|^2} \\ \hat{v} &= \hat{v}^* - k_2 \frac{(k_1\hat{u}^* + k_2\hat{v}^* + k_3\hat{w}^*)}{|\mathbf{k}|^2} \\ \hat{w} &= \hat{w}^* - k_3 \frac{(k_1\hat{u}^* + k_2\hat{v}^* + k_3\hat{w}^*)}{|\mathbf{k}|^2} \end{aligned} \tag{14}$$

Finally, the Fourier modes with a certain $|\mathbf{k}|$ are scaled so that the velocity field satisfies a prescribed energy spectrum $E(|\mathbf{k}|)$. Marstorp et al. (2005) used a high Reynolds number shape with the Kolmogorov inertial range slope $-5/3$ of the smallest resolved scales in their Large Eddy Simulations

$$E(|\mathbf{k}|) = \begin{cases} = k_p^{-11/3}|\mathbf{k}|^2 & |\mathbf{k}| \le k_p \\ |\mathbf{k}|^{-5/3} & |\mathbf{k}| > k_p \end{cases} \tag{15}$$

where k_p is the location of the peak, see figure 2. An additional scaling constant

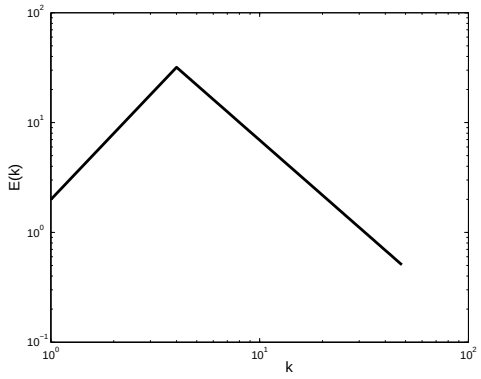

FIGURE 2. *The initial energy spectrum of the LES of Marstorp et al. (2005)*

is needed in order to specify the initial kinetic energy. The initial scalar field is without any fluctuations.

4. Summary

We have described a code for numerical simulation of homogeneous shear flow with a constant mean passive scalar gradient. The use of periodic boundary conditions requires a transformation to a frame that moves with the mean flow. The code uses a pseudo-spectral technique. All spatial derivatives are accurately calculated in Fourier space whereas the nonlinear terms are calculated in physical space. The aliasing errors that rises from the computation of the nonlinear terms are removed using a combination of truncation and phase shifts. The time advancement is performed in Fourier space using an explicit third order Runge Kutta method. The initial condition for the velocity field is random and isotropic with a prescribed shape of the energy spectrum and the initial scalar field is without any fluctuations.

References

Brethouwer G, Matsuo Y. 2005. DNS of rotating homogeneous shear flow and scalar mixing. Proc. 4th Int. Symp. on Turbulence and Shear Flow Phenomena (TSFP4), Williamsburg, USA. Editors: J A C Humphrey et al.

Marstorp L, Brethouwer G, Johansson A. 2005. Stochastic SGS modelling in rotating homogeneous shear flow with a passive scalar. To appear in *Proc. Direct and Large Eddy simulations 6 (DLES6)*, Poitiers, France.

Kang, H.S. ; Meneveau, C. 2001. Passive scalar anisotropy in a heated turbulent wake, new observations and implications for large eddy simulations *J. Fluid Mech.* **442**, 161-170.

Bardina J Ferzinger J.H Reynolds, W.C. 1983. Improved turbulence models based on large eddy simulation of homogeneous incompressible flows. Technical report No. **TF-19** Stanford University.

Rogallo, R. 1981. Numerical experiments in homogeneous turbulence. NASA Technical memorandum **81315**.

Rogers M M, Mansour N N, Reynolds W C. 1989. An algebraic model for the turbulent flux of a passive scalar. J. Fluid Mech. **203**, 77-101.

Rogers M M, Moin, P. 1987. The structure of the vorticity field in homogeneous turbulent flows J. Fluid Mech. **176**, 33-66.

Tavoularis S, Corrsin S. 1981. Experiments in nearly homogeneous turbulent shear flow with a uniform mean temperature gradient. Part 2. The fine structure, J. Fluid Mech. **104**, 349 - 367.

Williamson J. H. 1980. Low-Storage Runge-Kutta Schemes, J. Computational Physics. **35**, 48 - 56.